



Heat and continental transport shape the variability of volatile organic compounds in the Eastern Mediterranean: Insights from multi-year observations and regional modeling

5 Anchal Garg¹, Maximilien Desservettaz^{1,2}, Aliko Christodoulou^{1,3}, Theodoros Christoudias¹, Vijay Punjaji Kanawade¹, Chrysanthos Savvides⁴, Mihalis Vrekoussis^{1,5}, Shahid Naqui¹, Tuija Jokinen¹, Joseph Byron⁶, Jonathan Williams^{1,6}, Nikos Mihalopoulos^{1,7}, Eleni Liakakou⁷, Jean Sciare¹, and Efstratios Bourtsoukidis¹

¹Climate and Atmosphere Research Centre, The Cyprus Institute, Nicosia 2121, Cyprus

²Centre for Atmospheric Chemistry, University of Wollongong, Wollongong, NSW 2500, Australia

10 ³PSI, Center for Energy and Environmental Sciences, 5232 Villigen, Paul Scherrer Institute, Switzerland

⁴Department of Labour Inspection, Ministry of Labour and Social Insurance, Nicosia, Cyprus

⁵Institute of Environmental Physics, University of Bremen, Bremen, Germany

⁶Atmospheric Chemistry Department, Max Planck Institute for Chemistry, 55128, Mainz, Germany

15 ⁷Institute for Environmental Research and Sustainable Development, National Observatory of Athens, Palaia Penteli, 15236 Athens, Greece

*Correspondence: Anchal Garg (a.garg@cyi.ac.cy), Efstratios Bourtsoukidis (e.bourtsoukidis@cyi.ac.cy)

Abstract. Volatile organic compounds (VOCs) are key precursors in tropospheric ozone formation and secondary organic aerosol formation, thereby influencing regional air quality and climate. This study
20 investigates the seasonal, diurnal, and temperature-driven variability of VOCs at a rural background site in Cyprus, located in the Eastern Mediterranean. VOC measurements (April 2022 – June 2024) conducted with a proton transfer reaction time-of-flight Mass spectrometer (PTR-ToF-MS), along with HYSPLIT air mass back-trajectory analysis and WRF-Chem atmospheric chemistry simulations. Seventy-six VOCs were
25 quantified and categorized into classes such as oxygenated VOCs (OVOCs), aliphatic hydrocarbons, aromatic hydrocarbons, terpenes, and nitrogen- and sulfur-containing compounds. Most VOCs exhibited distinct diurnal cycles, observed highest during 08:00–14:00 UTC due to enhanced photochemical activity and temperature-driven emissions. Biogenic VOCs, particularly isoprene, peaked in summer within the 35–38 °C range but declined under extreme heat, suggesting emission suppression from thermal stress. Monoterpenes showed elevated levels both day and night, reflecting contributions from biogenic and
30 anthropogenic sources. Dimethyl sulphide (DMS) increased during warmer months, indicating enhanced marine microbial activity. OVOCs displayed strong seasonal and thermal enhancement during hot, dry summers due to both primary emissions and secondary formation. Benzene rose above 35 °C from evaporative and potential stress-related biogenic sources, whereas toluene and xylene were higher in colder months, linked to combustion processes. While WRF-Chem captured seasonal trends, most VOCs were
35 underestimated, highlighting missing emission sources and oxidation pathways. Overall, the study emphasizes temperature and regional transport as key drivers of VOC variability in the Eastern Mediterranean.



1 Introduction

40 Volatile Organic Compounds (VOCs) are a diverse group of carbon-based chemicals with high vapor pressures that play a central role in atmospheric chemistry (Atkinson, 2000; Kamal et al., 2016). Upon release into the atmosphere, VOCs participate in photochemical reactions that contribute to the formation of tropospheric ozone (O₃), aerosol precursors, and secondary organic aerosol (SOA), both of which have far-reaching implications for air quality, human health, and climate (Atkinson, 2000; Ehn et al., 2014; 45 Koppmann, 2020; Mellouki et al., 2015; Pennington et al., 2021; Wang et al., 2024). These compounds with lifetimes ranging from minutes to months originate from anthropogenic sources such as fossil fuel combustion, solvent use, industrial processes, and biogenic sources, including vegetation, soils, and marine emissions, and also emissions from biomass burning and wildfires (Atkinson, 2000; Bourtsoukidis et al., 2018; Capes et al., 2009; Civan et al., 2015; Debevec et al., 2017; Desservettaz et al., 2023; Huang et al., 50 2020; Kaltsonoudis et al., 2016; Pinthong et al., 2022; Pugliese et al., 2023; Ralf Koppmann, 2007; Sindelarova et al., 2014; Wang et al., 2022a; Yuan et al., 2024).

In scientific literature, these compounds are frequently classified into the broader categories of oxygenated VOCs (OVOCs), biogenic VOCs (BVOCs), and anthropogenic VOCs (AVOCs), each of the species with distinct sources, reactivities, and atmospheric lifetimes (Debevec et al., 2017; Koppmann, 2020; Yuan et al., 55 2024). OVOCs, including alcohols, aldehydes, ketones, organic acids, and others, are emitted directly from both anthropogenic and biogenic sources but are predominantly formed secondarily via the oxidation of primary VOCs by hydroxyl radicals (OH), O₃, and nitrate radicals (NO₃) (Huang et al., 2020; Mellouki et al., 2015; Wang et al., 2022b). These compounds are important intermediates in the photochemical formation of SOA and contribute to the oxidative capacity of the atmosphere over both local and regional scales (Huang 60 et al., 2020; Liu et al., 2009; Mellouki et al., 2015; Wang et al., 2020, 2022b). On the other hand, BVOCs such as isoprene, monoterpenes, and sesquiterpenes are emitted by vegetation through enzyme-driven processes influenced by environmental drivers (Bourtsoukidis et al., 2024, 2025; Brito et al., 2018; Ciccioli et al., 2023; Sindelarova et al., 2014; Wang et al., 2024). In the Mediterranean, pine and oak forests are major sources of BVOCs (Mecca et al., 2024; Song et al., 2011). AVOCs, comprising alkanes, alkenes, and 65 aromatic hydrocarbons, arise primarily from fossil fuel combustion, industrial operations, solvent use, biomass burning (both through direct emissions and secondary production) and vehicular traffic, with elevated levels observed in urban areas and near industrial and shipping activities (Atkinson, 2000; Civan et al., 2015; Kajos et al., 2015; Kaltsonoudis et al., 2016; Perrone et al., 2014; Sicre et al., 1987).

The eastern mediterranean and middle east (EMME) region is a climatically sensitive and chemically 70 dynamic region (Lazoglou et al., 2024; Zittis et al., 2022) owing to high solar radiation, elevated temperatures, and complex meteorology. The EMME experiences mixed air masses from Western and Eastern Europe, the Middle East, and North Africa, bringing emissions from industrial, biogenic, marine, and biomass burning sources (Bourtsoukidis et al., 2018; Germain-Piaulenne et al., 2024; Lelieveld et al., 2002; Traub et al., 2003). This convergence, combined with the increasing frequency of heatwaves (Lazoglou 75 et al., 2024), enhances biogenic and evaporative AVOCs emissions and hence, photochemical activity, raising



concerns over regional ozone and SOA formation. Cyprus, located at the core of this region, offers a unique setting to investigate these interactions.

80 Long-term measurements of VOCs in the EMME are scarce. At Finokalia, Greece, the studies of Liakakou et al., (2007, 2009) reported extended records of isoprene and C₂–C₈ hydrocarbons, while in Athens, the studies of Panopoulou et al., (2018, 2020) presented multi-year observations of isoprene, terpenes, and C₂–C₈ non methane hydrocarbons (NMHCs). In contrast to these gas chromatography-based observations, proton-transfer-reaction time-of-flight mass spectrometry (PTR-ToF-MS) studies in the region have thus far been limited to short-term, campaign-based deployments (Derstroff et al., 2017; Kaltsonoudis et al., 2016). Overall, despite extensive research in diverse regions, the understanding of VOCs variability and drivers in
85 the EMME region remains limited, particularly in terms of long-term and multi-year observations that can capture seasonal and climate change-driven dynamical responses to extreme heat.

Addressing this gap, the current study presents multi-year high-resolution VOCs measurements collected from 2022 to 2024 at a rural background site in Cyprus located in EMME region. Using PTR-ToF-MS, we quantified 76 VOC species across biogenic, anthropogenic, and oxygenated classes. To identify regional
90 contributions, we apply hybrid single-particle lagrangian integrated trajectory (HYSPLIT) airmass back-trajectory analysis and examine air mass origins across seven distinct geographical sectors. Furthermore, we evaluated selected VOC species simulated by the weather research forecast model coupled with chemistry (WRF-Chem) model which includes a high-resolution mapping of local emissions (Georgiou et al., 2022). This integrated approach enables us to (i) characterize diurnal and seasonal VOCs patterns, (ii) assess the
95 influence of temperature on VOCs composition and chemical processing, (iii) understand key emission sources, (iv) evaluate the impact of long-range transport on VOCs variability, and (v) assess the model performance in the estimation of VOCs.

2 Methodology

2.1 Study area and VOCs measurement timeline

100 Cyprus, the third-largest island in the Mediterranean, is situated at the air pollution crossroads of Europe, Asia, and Africa, making it a receptor for long-range atmospheric transport from diverse source regions (Lelieveld et al., 2002). Air masses influencing the island originate from Western and Eastern Europe, Turkey, North Africa, Southwest and Northwest Asia, the Middle East, and the surrounding Mediterranean Sea (Fig. 1a). This convergence of continental and marine influences makes Cyprus an ideal location for
105 investigating the chemical complexity of both long-range transported and local air pollutants (Meusel et al., 2016; Derstroff et al., 2017; Debevec et al., 2017; Vrekoussis et al., 2022).

The present study was conducted at the Cyprus Atmospheric Observatory – Agia Marina Xyliatou (CAO-AMX, 35.0387° N, 33.0579° E), located at 532 m above sea level at the foothills of the Troodos Mountains (Fig. 1b–c). Established in 1997 and upgraded in 2015 to a “supersite,” CAO-AMX provides high-quality,
110 long-term measurements of aerosols and their properties, greenhouse gases, meteorological parameters, and



115 trace gases. It is designed and operated as a rural background site (CAO-AMX, <https://cao.cyi.ac.cy/>)
primarily by the climate and atmosphere research center (CARE-C) of the Cyprus institute (Cyl), in
collaboration with national authorities such as the department of labour inspection (DLI) of the ministry of
labour and social insurance, while it is part of major international atmospheric monitoring networks,
including ACTRIS (<https://www.actris.eu/>); EMEP (<https://www.emep.int/>); and AERONET
120 (<https://aeronet.gsfc.nasa.gov/>) (Sciare J, 2016). The station is situated near the small villages of Agia Marina
(~630 inhabitants) and Xyliatos (~150 inhabitants), surrounded by oak-pine forests and Maquis shrubland,
with agricultural fields ~4 km to the north (Baalbaki et al., 2021). The nearest urban area lies >35 km away,
ensuring minimal influence from local pollution sources aside from limited vehicle traffic. Its rural setting,
surrounded by forested and low-population areas and situated far from major urban sources (Nicosia about
125 35 km to the northeast and Larnaca about 50 km to the southeast) ensures that measurements are minimally
influenced by major nearby local anthropogenic emissions. This allows the observation of representative
background concentrations and the signatures of regional and long-range transported pollutants.
The VOCs observations were conducted from April 27, 2022, to June 15, 2024, with occasional interruptions
caused by field campaigns or instrument downtime. As shown in Fig. 1d, monthly data coverage varied but
provided efficient coverage across all seasons. Fig. 1e summarizes the seasonal and annual distribution of
data points: summer (32%) was the most represented season, followed by spring (30%) and autumn (23%),
while winter accounted for 15% of the data. In terms of annual contribution, 2022 comprised 44% of the
total dataset, 2023 contributed 25%, and 2024 contributed 31%.

130 2.2 VOCs measurements

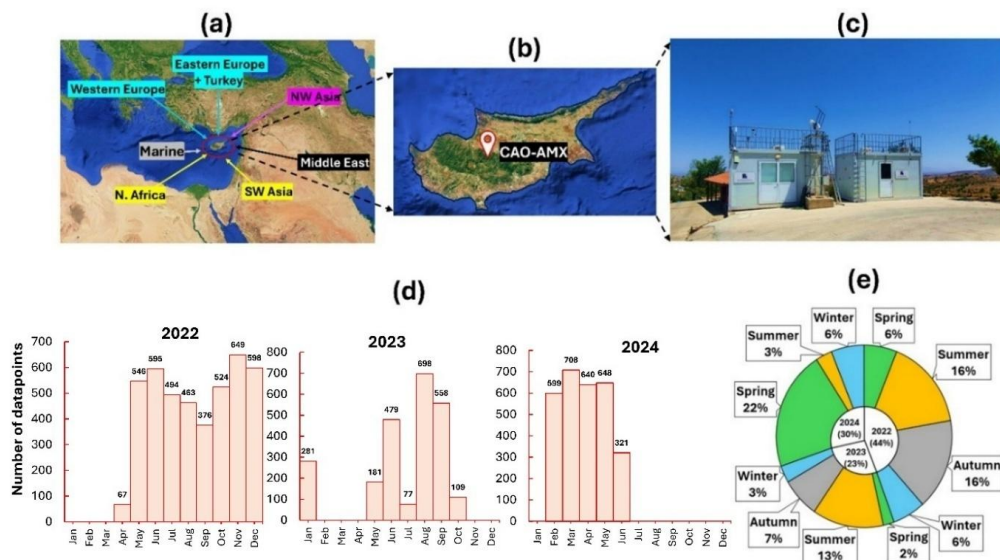
Online measurements of VOCs were performed using a high-resolution PTR-ToF-MS (Model: 4000; Ionicon
Analytik GmbH, Innsbruck, Austria) following the methodology as described by Desservettaz et al., (2023).
Briefly, the drift tube of the PTR-ToF-MS was operated under controlled conditions with an electric field to
number density ratio (E/N) of 128 Townsend (Td), a pressure of 2.2 mbar, an applied voltage of 630 V, and
135 a temperature of 85 °C. Ambient air was sampled at a flow rate of 210 mL min⁻¹ through a 2.0 m long, 1/16”
PEEK (polyether ether ketone) heated inlet line, equipped with a 0.45 µm PTFE particulate filter (PALL,
USA). The inlet drew air from a common glass manifold shared with other atmospheric measurement
instruments. The use of chemically inert materials such as PTFE and PEEK minimized potential compound
losses within the sampling line.

140 The instrument was automatically switched to measure VOC-free air for 20 minutes after every 23 hours,
followed by 40 minutes of calibration using a certified gas standard (Apel-Riemer Environmental, USA)
containing major VOCs diluted to ~20 ppbv, to establish baseline levels. Mass spectra were acquired at 1-
minute time resolution and averaged to 1-hour intervals for the analysis in this study. The instrument
sensitivity was interpolated between calibrations and adjusted for humidity dependence based on water
145 cluster ion ratios. Calibrated sensitivities showed modest temporal variability (~10-23%) for most
compounds.



150
155
160

Post-acquisition analysis was carried out using the Ionicon data analyzer (IDA), with mass axis calibration based on H_3O^+ and internal reference peaks (e.g., $\text{C}_6\text{H}_5\text{I}^+$). The software retrieved exact masses and chemical formulas for ~1200 peaks, of which 400–500 was assigned tentative structures using the GLOVOCS database, which is a master compound assignment guide that can be referred to as PTR-MS practitioners (Yáñez-Serrano et al., 2021). A set of 131 common species across analysis periods was further corrected using transmission curves derived from zero and calibration air sampling. Mixing ratios (ppbv) were calculated from ion counts, incorporating species-specific reaction rate constants (k-values) based on molecular dipole moments and polarizabilities (Desservettaz et al., 2023; Pagonis et al., 2019). The limit of detection (LOD) for each species was defined as three times the standard deviation observed during zero-air measurements and averaged over the entire campaign. VOC species with more than 30% of their data below the LOD were excluded, resulting in a final dataset of 76 species, with sub-LOD concentrations appropriately flagged. Measurements impacted by filter changes, exhibiting short-term interference (notably acids and certain hydrocarbons), were filtered by removing a conservative 2-hour window following each swap. Formaldehyde was not included in this study due to its inconsistent identification by the IDA software during part of the measurement period. Furthermore, quantification of formaldehyde via PTR-based techniques is known to be highly sensitive to humidity variations (Vlasenko et al., 2010), which complicates reliable detection. Accurate quantification would require water-dependent calibrations and a dedicated formaldehyde calibration standard, conditions that were not met during the measurement period.



165
170

Figure 1: Geographic context, air mass origins, and VOC measurement coverage at the CAO-AMX site (2022–2024). (a) Major regional air mass source areas influencing Cyprus; (b) Location of the CAO-AMX in the Troodos Mountains; (c) The CAO-AMX monitoring station, a designated regional background site; (d) Monthly distribution of number of datapoints for VOC measurements from April 2022 to June 2024; (e) Summary of data coverage by season and year, showing overall representativeness of the dataset for multi-seasonal and multi-annual analysis.



2.3 Meteorological and air pollutant data

Meteorological and auxiliary air quality parameters were analyzed to provide contextual insight into atmospheric dynamics and pollutant characteristics. Meteorological data were recorded at a temporal resolution of 5 minutes from a dedicated station located in the village of Xyliatos (35.0141° N, 33.0492° E), approximately 2.85 km from the primary observational site at the CAO-AMX. The meteorological station, positioned at 10 meters above ground level, continuously measured key atmospheric variables, including ambient temperature (AT), relative humidity (RH), solar radiation (SR), wind speed (WS), and wind direction (WD). DLI managed the installation and operation of a relatively dense monitoring network at this station. In addition, a range of trace gases and particulate pollutant levels were measured at a co-located air quality monitoring station, operating under the European monitoring and evaluation programme (EMEP) framework. This station, situated approximately 20 meters from the main VOC measurement container, provided hourly-resolved concentrations of major atmospheric pollutants: ozone (O₃), carbon monoxide (CO), nitrogen oxides (NO, NO₂, and NO_x), sulfur dioxide (SO₂), and particulate matter with aerodynamic diameters less than 10 μm (PM₁₀) and 2.5 μm (PM_{2.5}). These measurements serve as critical auxiliary data for assessing the chemical background of the region, evaluating pollutant transport processes, and validating model simulations. Instrument specifications, calibration protocols, and operational details of the meteorological and air quality monitoring systems are extensively documented in previous studies (Kleanthous et al., 2014; Pikridas et al., 2018; Vrekoussis et al., 2022).

2.4 HYSPLIT backward trajectory

To assess the influence of long-range atmospheric transport on local air quality, five-day back trajectories were computed using the HYSPLIT model (version 4.4; Draxler, 1997; Stein et al., 2015). These calculations were performed using the PC-based version of HYSPLIT provided by the national oceanic and atmospheric administration's (NOAA) air resources laboratory (ARL), incorporating meteorological data from the global data assimilation system (GDAS) with a spatial resolution of 1° × 1° and a temporal resolution of 1-hour (Draxler, 1997). Trajectories were initialized every hour at an altitude of 500 m above ground level (AGL), and each point along the trajectory was calculated at a one-hour time step. The air mass trajectory cluster analysis, following the methodology previously applied by Debevec et al., (2017) identified a total of seven air mass clusters: (C0) slow-moving or stagnant local air masses, (C1) North Africa, (C2) Marine-influenced, (C3) Europe, (C4) Northwest Asia, (C5) West Turkey, and (C6) Middle east origins. For the cluster analysis, the altitude of the end point was set at 1000 m AGL for each trajectory (Debevec et al., 2017).

2.5 WRF-Chem model configuration for VOC simulation in Cyprus

To assess VOCs variability and compare modeled and observed mixing ratios over Cyprus, we employed the WRF-Chem model as described and evaluated in Georgiou et al. (2022). The setup used three nested domains with horizontal resolutions of 50, 10, and 2 km, the later focusing on Cyprus, with meteorological inputs from the global forecast system (GFS) every 3 hours. Key parameterizations included YSU for the boundary



layer, Noah land surface model (LSM) for land surface processes, the rapid radiative transfer model for global applications (RRTMG) for radiation, the regional atmospheric chemistry mechanism (RACM) for gas-phase chemistry and MADE/VBS for aerosols as described in (Georgiou et al., 2022). Photolysis was calculated using Fast-J. Anthropogenic emissions were sourced from emissions database for global atmospheric research-hemispheric transport of air pollution (EDGAR-HTAP) version 2 emission inventory. while BVOCs were simulated online using the Model of Emissions of Gases and Aerosols from Nature version (MEGAN) version 2.1 based on weather and land use data (Guenther et al., 2012).

For the innermost domain, a high-resolution emission inventory developed by (Georgiou et al., 2020) is used. This emission inventory uses the total reported emissions of CO, NO_x, non-methane VOCs (NMVOCs), SO₂, and PM on a 1 km × 1 km resolution (Georgiou et al., 2020) which is upscaled to the resolution of the innermost domain of the simulations (2 km) using a nearest-neighbor grid-point attribution algorithm, while diurnal, weekly, and monthly emission cycles are applied to each species and the predominant emission activity per season according to the (Schaap et al., 2011). The high -resolution emission inventory was found to adequately simulate of the daily profiles of NO_x and O₃ at measurement sites over Cyprus, and compared to CAMS, the WRF-Chem model predicts more accurately NO₂ mixing ratios with 7% during winter and -44 % during summer normalized mean bias during winter/summer, compared to -81% and -84% biases for the CAMS ensemble using the CAMS inventory (Georgiou et al., 2022).

In the outer model domain, the EDGAR emission inventory is used. In comparison with other emission inventories for VOCs, EDGAR provides a larger estimate than the EMEP emission inventory. The CAMS-REG-AP inventory also gives a smaller estimate, in comparison to EMEP. Comparing the VOC by the EDGAR inventory to the EMEP inventory, the higher emission estimates are greatest over Belgium, Austria, Switzerland, Germany and Finland, with differences mainly encountered in the industrial combustion sector and fugitive emissions. Regarding the modelled O₃ concentrations over Europe, all emission inventories were shown to show very similar patterns despite the noted differences in terms of emissions, particularly VOCs, indicating a low sensitivity to VOC emissions (Thunis et al., 2021).

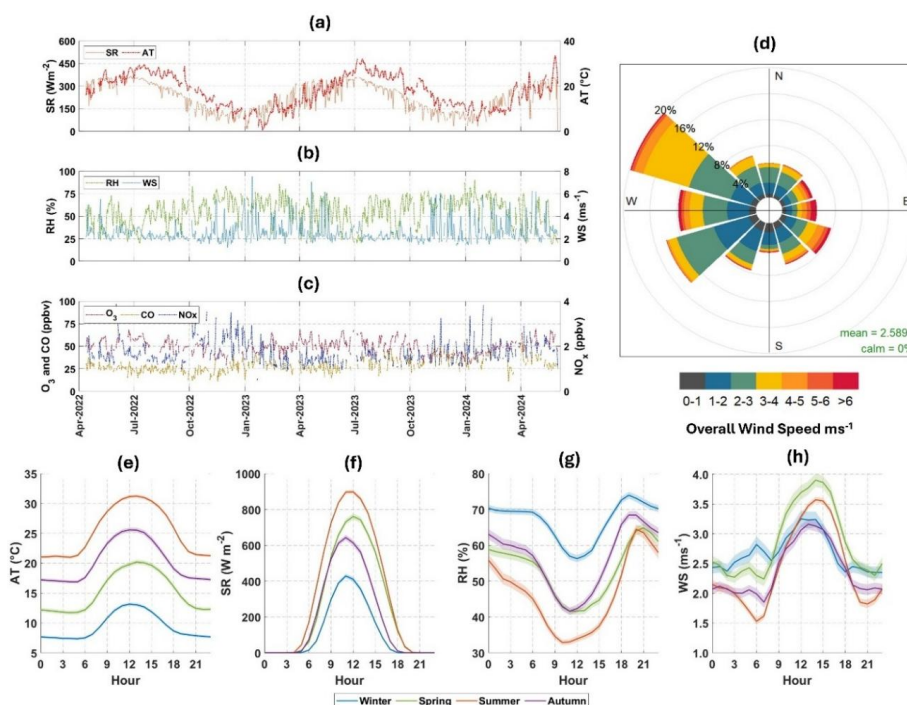
Major VOC species such as isoprene, monoterpenes, and aromatics were explicitly modeled. Outputs at hourly resolution were validated against PTR-ToF-MS measurements from CAO-AMX, enabling robust interpretation of VOC sources and atmospheric transport in the eastern mediterranean. The VOCs included in this study are based on the RACM (Stockwell et al., 1997) and encompass key anthropogenic and biogenic compounds relevant to regional air quality. These include isoprene (ISO), monoterpenes represented by α -pinene and related monocyclic terpenes with a single double bond (API), and d-limonene, along with other cyclic dienes (LIM). Aromatic compounds are grouped as toluene (TOL), which includes toluene and less reactive aromatics, and xylene (XYL), representing xylene and more reactive aromatic species. OVOCs are categorized as aldehydes (ALD), including acetaldehyde and higher molecular weight aldehydes, ketones (KET), and glyoxal (GLY).



3 Results and Discussion

3.1 Meteorological and atmospheric composition variability

245 Mean meteorological conditions included a WS of $2.6 \pm 1.4 \text{ m s}^{-1}$, RH of $55 \pm 20\%$, AT of $17.7 \pm 7.9 \text{ }^\circ\text{C}$, and
SR of $224.75 \pm 305.85 \text{ W m}^{-2}$ (Fig. 2a). Average AT ($\sim 35 \text{ }^\circ\text{C}$) and SR ($>600 \text{ W m}^{-2}$) peaked in summer, while
winter had the lowest values ($\sim 5 \text{ }^\circ\text{C}$ and $\sim 200 \text{ W m}^{-2}$ Fig. 2e-f). RH showed the opposite pattern ($\sim 85\%$ in
winter, $<30\%$ in summer) (Fig. 2g). Midday peaks in temperature and radiation were strongest in summer,
with RH lowest in the afternoon (Fig. 2e-g). RH and SR were inversely correlated, consistent with previous
studies (Emekwuru and Ejohwomu, 2023; Matthew, 2022). Daily average WS ranged from 1 to 4 m s^{-1} , with
250 slightly higher values observed in spring and summer, suggesting enhanced mixing during these periods
(Fig. 2h). Diurnal patterns were also pronounced as WS showed afternoon maxima in all seasons, with
enhanced values in spring and summer, likely driven by thermal convection and sea breeze circulation (Fig.
2h), promoting more effective dispersion of air pollutants (Deot et al., 2025; Pérez et al., 2020; Soukissian
and Sotiriou, 2022).



255

260

Figure 2: Seasonal and diurnal variability of meteorological parameters and air pollutants in Cyprus. Panels (a–c) show time series (24-hour rolling average) of (a) ambient temperature (AT) and solar radiation (SR), (b) relative humidity (RH) and wind speed (WS), and (c) gaseous pollutants, including ozone (O_3), carbon monoxide (CO), and nitrogen dioxide (NO_2) for study period. Panel (d) displays wind rose diagrams indicating wind speed and direction for the entire study period. Panels (e–h) present the diurnal profiles of (e) ambient temperature ($^\circ\text{C}$), (f) solar radiation (W m^{-2}), (g) relative humidity (%), and (h) wind speed (m s^{-1}) across the four seasons (spring, summer, autumn, winter). Shaded regions in panels (e–h) represent the standard error, capturing variability in diurnal cycles.



265 Wind analysis throughout the study period revealed predominantly moderate conditions, with over 70% wind speeds falling below 3 ms^{-1} , and 94% below 5 ms^{-1} . The wind rose diagrams (Fig. 2d) highlight the prevalence of moderate-speed winds and dominant directions ranging from northwesterly to west-southwesterly. Fig. S1 shows seasonal and monthly variability in wind direction, and suggests that during the winter, the winds were mainly coming from the southeast, followed by the southwest, with most wind speeds exceeding 4 ms^{-1} ; whereas, for the other seasons, the winds originated predominantly from the northwest.

270 Atmospheric conditions were characterized by the following mean mixing ratios for gaseous pollutants such as NO at $0.3 \pm 0.2 \text{ ppbv}$, NO_2 at $1.4 \pm 0.8 \text{ ppbv}$, NO_x at $1.7 \pm 0.9 \text{ ppbv}$, SO_2 at $0.5 \pm 0.4 \text{ ppbv}$, O_3 at $49.2 \pm 9.0 \text{ ppbv}$, and CO at $145.8 \pm 49.5 \text{ ppbv}$. During daytime O_3 remained consistently elevated throughout the year, with a significant increase of (8-20 ppbv) of its mixing ratio in summer, indicating a strong influence from regional transport and photochemical formation (Kleanthous et al., 2014; Lee et al., 2021; Pochanart et al., 2003). A notable increase in CO levels was observed between 2022 and 2024. A modest rise in CO observed during winter is likely due to increased combustion emissions, lower sink due to low photochemistry, variable residence time of upto 90 days in winter and 30 days in summer, and weaker atmospheric dispersion (Koppmann et al., 2005; Pochanart et al., 2003). NO_x showed a winter maximum, consistent with increased anthropogenic emissions and reduced photochemical degradation (Atkinson, 2000; Civan et al., 2015; Koppmann et al., 2005).

3.2 Overview of atmospheric VOCs observations

285 A total of 76 VOCs were quantified, and their descriptive statistics for key species are summarized in Table 1, while the complete list is provided in supplementary Table S1. These VOCs were grouped into six major chemical classes: (i) OVOCs, including alcohols, carbonyls, organic acids, and other oxygenates; (ii) aliphatic hydrocarbons; (iii) aromatic hydrocarbons; (iv) terpenes; and (v) nitrogen- and sulfur-containing VOCs (N & S containing VOCs). An overview of the average mixing ratios is shown in Fig. 3, while Fig. S2 illustrates the time series of selected VOCs. OVOCs were the dominant chemical class as observed by Debevec et al., 2017, contributing approximately 79% to the total measured VOC burden. Among these, alcohol was the most abundant subgroup, comprising 32% of total VOCs. Methanol was the single most dominant species, with a median mixing ratio of 2.86 ppbv, accounting for 87% of the total alcohol fraction. Its high dominance reflects oxidation of biogenic and biomass burning emissions, consistent with previous findings (Debevec et al., 2017; Mukherjee et al., 2024; Yuan et al., 2024). Carbonyl compounds represented the second largest OVOCs subgroup (28% of total VOCs), with median levels dominated by acetone (2.11 ppbv, 74% of the carbonyl group), followed by acetaldehyde (0.54 ppbv, 19% of the carbonyl group). These compounds are known to originate from both primary sources and secondary oxidation of VOCs (Capes et al., 2009; Mellouki et al., 2015; Mukherjee et al., 2024; Pennington et al., 2021; Wang et al., 2024, 2022b). Elevated levels during summer (Fig. 2b) suggest increased biogenic activity and enhanced photochemical production.



300 Organic acids, primarily acetic acid (0.68 ppbv) and formic acid (0.42 ppbv) contributed 13% of total VOCs,
which could mainly arise from biogenic emissions, anthropogenic emissions and secondary photochemical
oxidation of VOCs (Derstroff et al., 2017; Huang et al., 2020; Kamal et al., 2016; Koppmann, 2020; Wang
et al., 2024, 2022b). Other oxygenates, such as methyl ethyl ketone (MEK) and acrolein, also contributed to
the OVOCs group and may originate from industrial sources and atmospheric oxidation (Schieweck et al.,
2021; Torres-Vinces et al., 2020; Yáñez-Serrano et al., 2016). Aliphatic hydrocarbons accounted for 12% of
305 total VOCs, with species such as propylene, propyne, 1,3-butadiene, and cyclohexadiene likely reflecting
emissions from vehicular traffic, fossil fuel combustion and industrial activities (Perrone et al., 2014; Sicre
et al., 1987). Aromatic hydrocarbons, though less abundant (3%), were dominated by benzene (0.14 ppbv,
32% of the aromatic fraction), followed by toluene and xylene. These compounds are well-known tracers of
urban and industrial emissions (Abbasi et al., 2020; Boutsoukidis et al., 2019; Boutsoukidis et al., 2020;
310 Das et al., 2024), though their overall concentrations were low, consistent with the remote and background
nature of the site.

The primary BVOCs mainly include terpenes, such as monoterpenes (median= 0.27 ppbv) and isoprene
(median= 0.09 ppbv), collectively contributing ~3% of the VOC budget. Their mixing ratio peaked in
summer, aligning with increased biogenic emissions driven by higher temperatures and SR (Gu et al., 2021;
315 Liakakou et al., 2007; Mukherjee et al., 2024; Sindelarova et al., 2014; Strada et al., 2023; Wang et al., 2024).
N & S containing VOCs also contributed approximately 3%, with median acetonitrile (0.11 ppbv) and
dimethyl sulfide (DMS, 0.04 ppbv) mixing ratios as the major constituents. Acetonitrile, a tracer for biomass
burning, accounted for 40% of this group, while DMS reflects both marine and biological sources
(Deschaseaux et al., 2022; Edtbauer et al., 2020; Huangfu et al., 2021; Robles, 2005).

320 The analysis of the 20 most abundant VOCs (Fig. S3) also reinforced the dominance of OVOCs, particularly
methanol, acetone, and acetic acid, which together formed a substantial fraction of the observed VOC mass.
The relatively low levels of aromatics and aliphatic further support the interpretation that this rural
background site is primarily influenced by transported VOC precursors, secondary atmospheric processes
and regional-scale transport, rather than direct anthropogenic emissions.

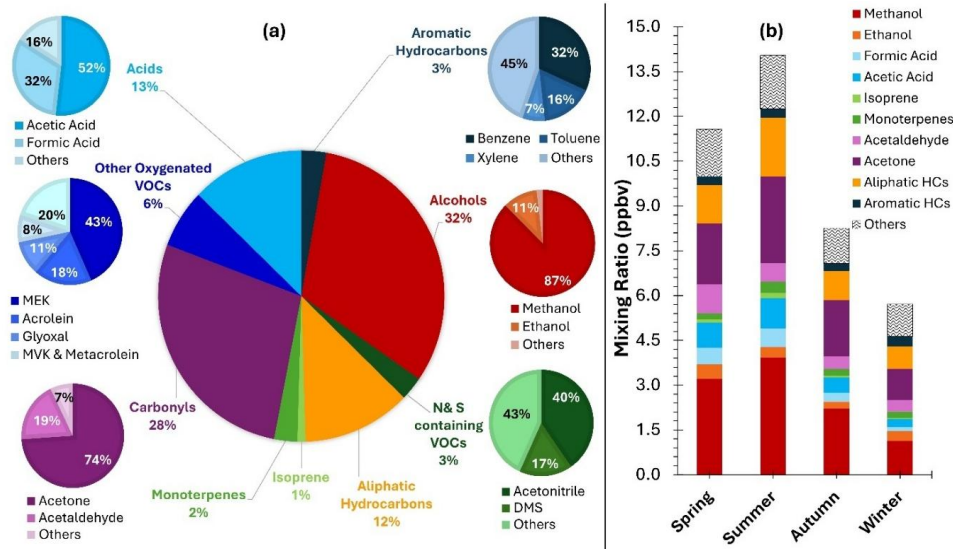
325 **Table 1. Descriptive statistics of selected VOCs (in ppbv) measured in Cyprus (April 2022- June 2024)**

Chemical Name	Chemical Formula	Group	M.H ⁺	Min	Max	Mean	Median	SD
Methanol	CH ₄ O	Alcohol	33.03	0.138	27.82	3.08	2.86	1.71
Acetonitrile	C ₂ H ₃ N	N	42.04	0.041	0.33	0.12	0.11	0.04
Acetaldehyde	C ₂ H ₄ O	Aldehyde	45.03	0.123	6.76	0.88	0.54	0.89
Formic Acid	CH ₂ O ₂	Acids	47.01	0.022	7.99	0.78	0.42	0.93
Ethanol	C ₂ H ₆ O	Alcohol	47.05	0.009	3.68	0.43	0.35	0.35
Acrolein	C ₃ H ₄ O	Oxygenated	57.03	0.01	1.93	0.2	0.12	0.23
Glyoxal	C ₂ H ₂ O ₂	Oxygenated	59.01	0.019	1.22	0.07	0.07	0.04
Acetone	C ₃ H ₆ O	Ketone	59.05	0.429	10.82	2.35	2.11	1.19
Acetic Acid	C ₂ H ₄ O ₂	Acids	61.03	0.039	12.54	1.25	0.68	1.56



DMS	C ₂ H ₆ S	S	63.04	0.005	0.55	0.06	0.04	0.06
Furan	C ₄ H ₄ O	Oxygenated	69.03	0.004	0.16	0.01	0.01	0.01
Isoprene	C ₅ H ₈	Biogenic	69.07	0.005	2	0.15	0.09	0.18
MVK/Methacrolein	C ₄ H ₆ O	Oxygenated	71.05	0.003	0.53	0.08	0.06	0.07
MEK	C ₄ H ₈ O	Oxygenated	73.07	0.007	2.78	0.36	0.29	0.27
Benzene	C ₆ H ₆	Aromatics	79.05	0.018	1.09	0.16	0.14	0.11
Toluene	C ₇ H ₈	Aromatics	93.07	0.005	1.3	0.1	0.07	0.1
Xylene	C ₈ H ₁₀	Aromatics	107.09	0.003	1.76	0.06	0.03	0.12
Monoterpenes	C ₁₀ H ₁₆	Biogenic	137.13	0.026	3.01	0.34	0.27	0.27

Compounds are grouped by chemical class, with molecular hydrated ion mass (M.H⁺) shown for each. These data provide insight into the variability and typical concentrations of VOCs in the region, relevant to air quality and atmospheric chemistry assessments.



330 **Figure 3: Overview of VOCs in Cyprus: Composition and seasonal variability in its composition.** (a) % contribution of different VOC groups in Cyprus, highlighting the dominance of alcohols (32%), carbonyls (28%), and acids (13%). Subcategories within each VOC group are detailed in smaller pie charts. (b) Seasonal variability of the VOCs mixing ratio.

335 As shown in Table 2, VOC mixing ratios measured in our study are within the range reported from other European background and rural sites. Winter mixing ratios for acetaldehyde, acetone, MVK, MEK, acetonitrile, benzene, isoprene, and monoterpene were also comparable to those measured during the same period in 2015 at this site (Debevec et al., 2017), suggesting stable background concentrations and low interannual variability in the Eastern Mediterranean. However, summertime isoprene mixing ratios at Ineia, Cyprus, were about three times lower. Derstroff et al. (2017) demonstrates potential contribution of
 340 downwind forest emissions or the effect of hotter summers and stress induced emissions.



Table 2. Seasonal mean mixing ratios (ppbv) of VOCs measured in our study compared with previous regional and European studies.

Location	Measurement	Study Reference	Year, Season	Terpenes				Aromatics				Oxygenated			Nitrile	
				Isoprene	Mono-terpenes	Benzene	Toluene	Xylene	Methanol	Ethanol	Acetic Acid	Acetaldehyde	Acetone	MVK+ Methacrolein	MEK	Acetonitrile
CAO, Cyprus (Background)	PTR-ToF-MS	This study	Spring 2022-24	0.12	0.20	0.14	0.06	0.03	3.22	0.47	0.84	0.97	2.03	0.06	0.35	0.10
			Summer 2022-24	0.18	0.39	1.30	0.07	0.03	3.92	0.35	1.00	0.61	2.90	0.09	0.28	0.13
			Autumn 2022-24	0.06	0.23	0.12	0.06	0.02	2.22	0.23	0.52	0.42	1.90	0.04	0.24	0.12
			Winter 2022-24	0.03	0.22	0.15	0.09	0.04	1.14	0.33	0.27	0.39	1.05	0.03	0.29	0.08
CAO, Cyprus (Background)	PTR-MS, GC-MS	Debeves et al., 2017	Winter, 2015	0.05	0.24	0.12	0.05	0.02	2.93		0.41	1.15	0.03	0.22	0.12	
			Summer, 2014	0.06	0.11	0.02	0.01	0.02	2.90		0.95	0.32	2.25	0.03	0.11	0.11
Zürich, Switzerland (Urban background)	GC-MS	Legreid et al., 2007	Spring 2005	0.08		0.41	1.46	0.97	2.18	6.87		1.66	0.04	0.24		
			Summer 2005	0.16		0.23	1.43	0.83	3.18	3.94		2.12	0.12	0.20		
			Autumn 2005	0.08		0.48	1.70	1.10	1.11	7.61		0.45	1.24	0.04	0.17	
			Winter 2005	0.06		0.75	1.25	0.91	1.21	7.53		0.82	1.17	0.05	0.22	
Athens, Greece (urban)	PTR-MS	Kaltsonoudis et al., 2016	Summer 2012	0.73	0.92	0.22	0.81	0.67	1.52	2.17	4.28	0.35	0.50	0.20		
			Winter 2013	1.05	0.43	1.00	2.34	1.69	1.80	2.11	2.24	0.41	0.59	0.16		
Cape Corsica, France (urban)	PTR-MS	Michoud et al., 2017	Summer 2013	0.19	0.41	0.03	0.08		0.18		3.43	0.06	0.48			
			Spring 2012	1.19	0.06	0.07	0.05		2.28		0.38	1.28	0.21			
Mediterranean Forest, France	PTR-MS	Secco et al., 2011	Summer	0.15-0.75	0.13-1.42	0.04-0.09	0.08-0.47	0.08-0.09	4.14-6.05	1.15-2.87	1.32-2.94	0.54-1.26	2.26-3.83	0.17-0.54	0.16-0.22	
			Winter	0.02-0.07	0.005-0.067	0.11-0.19	0.06-0.41	0.06-0.41	1.28-2.70	0.47-2.08	0.39-1.43	0.79-1.55	0.01-0.05	0.08-0.10		
			Spring 2022	0.04	0.05	0.14	0.47		3.50		0.92	1.93	0.09	0.22	0.41	
			Summer 2022	0.18	0.19	0.08	0.80		3.73		0.31	2.50	0.17	0.24	0.29	
Montseny, Spain (rural background)	PTR-ToF-MS	Iri't Veld et al., 2024	Spring 2022	0.05	0.02	0.13	0.22		1.46		0.48	1.02	0.05	0.19	0.10	
			Summer 2022	0.30	0.45	0.04	0.09		3.89		0.84	2.76	0.55	0.30	0.12	
Oak (Mediterranean Forest, Spain)	PTR-MS	Yáñez-Serrano et al., 2021	Summer 2019	0.42	0.15	0.04	0.13		4.60		0.77	2.08	0.30	0.29	0.12	
			Autumn 2019	0.09	0.09	0.04	0.21		1.60		0.30	1.37	0.08	0.27	0.06	



345 Generally, the Mediterranean forested sites in France and Spain are characterised by higher daily
mean isoprene levels up to 1 ppbv (Kalogridis et al., 2014; Seco et al., 2011), consistent with strong
direct emissions from oak-dominated ecosystems compared to the conifer-dominated forest in
Cyprus. The urban site of Zurich, Switzerland shows similar seasonal pattern as our study, where
isoprene, methanol, acetone, and MVK all showed a summer maximum and a winter minimum
350 (Legreid et al., 2007). However, wintertime aromatic (BTX) concentrations were much higher in
Zurich presumably due to combustion sources related to anthropogenic activities. Nitriles and MEK
concentrations in our study fall in the range of those reported for previous European background
studies and confirm their regional well-mixing as resulting from both anthropogenic and biomass-
burning sources.

355 **3.3. Seasonal and diurnal variability of VOCs functional groups**

The diurnal variation of total VOCs (TVOCs) across all seasons and years (Fig. S4) reveals clear
patterns influenced by temperature, photochemistry, boundary layer dynamics, and emission
sources. TVOCs mixing ratio typically observed high between 09:00-14:00 UTC, corresponding to
enhanced daytime emissions and increased atmospheric reactivity. The highest median TVOCs
360 mixing ratios were observed during summer 2024 (25.76 ppbv), followed by summer 2023 (16.27
ppbv), spring 2024 (13.71 ppbv), and summer 2022 (12.35 ppbv), whereas winter exhibited the
lowest levels (5.83 ppbv). These results underscore the influence of photochemical processes and
temperature-driven biogenic emissions during warmer months, with the extreme heatwave in June
2024 likely intensifying VOCs release. During summer, there is also northerlies that promote the
365 transport of species from regions with pronounced anthropogenic emissions, including biomass
burning. Additionally, northerlies may bring pollution from north Cyprus (Vrekoussis et al., 2022).
Also, June 2024 was the hottest ever recorded in Cyprus, with multiple daily maximum temperature
records broken across the island (Cyprus Mail, 2024). The prolonged heat was attributed to a
persistent heatwave influenced by global climate change, with such extreme events forecasted to
370 become more frequent and intense in the future (Yáñez-Serrano et al., 2016; Zittis et al., 2022). Fig.
4 presents the diurnal profiles of VOCs for multiple seasons (2022–2024), which demonstrate
pronounced variability on seasonal and diurnal dynamics, particularly during summer 2024, when
elevated temperatures significantly enhanced VOCs levels across most chemical classes.

3.3.1. Terpenes (isoprene and monoterpenes)

375 High isoprene levels occurred during 08:00-14:00 UTC in summer 2023 and 2024, correlating with
peak SR and AT most of the time. In summer 2024, the median isoprene mixing ratio reached
approximately 1.0 ppbv during the day, with daily average median values of 0.43 ± 0.36 ppbv, while
monoterpenes showed broader diurnal presence, with early morning and evening peaks in some
seasons, and a summer median of 0.51 ± 0.20 ppbv. Interestingly, the observed isoprene maximum
380 at 08:00 UTC does not coincide with the peaks in SR and AT. This suggests that under the extreme
drought conditions of 2023 and 2024, vegetation may have downregulated photosynthesis unusually
early in the day. Such an early shutdown indicates that a physiological threshold was crossed,



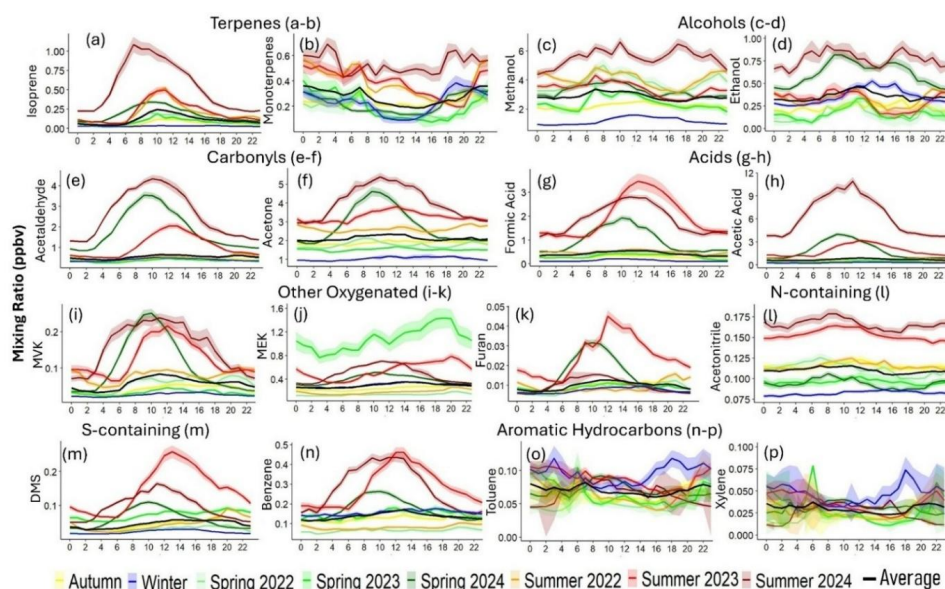
385

390

395

400

whereby plants shift their carbon allocation strategy from growth toward survival. While drought stress is often associated with an initial increase in isoprene emissions (Byron et al., 2022), prolonged or severe stress can suppress photosynthesis and consequently reduce isoprene release (Potosnak et al., 2014; Byron et al., 2022). Isoprene and monoterpenes exhibited distinctly different temporal patterns, reflecting their contrasting emission drivers and atmospheric dynamics. The seasonal pattern in isoprene align with established findings, where approximately 77% of annual emissions occur in spring (31%) and summer (46%), driven by elevated light intensity and temperature, which activate isoprene synthase enzymes (Fortunati et al., 2008; Monson et al., 1992). Autumn and winter emissions are markedly lower due to reduced photosynthetic activity and enzymatic downregulation (Panopoulou et al., 2020). Monoterpenes, while also of biogenic origin, demonstrated a more even seasonal distribution, with 38% of levels occurring in summer and 19–22% across other seasons. This distribution reflects not only temperature dependence but also anthropogenic and ecological responses to herbivory, wounding, and water stress, particularly relevant under changing climate conditions (Bourtsoukidis et al., 2025; Peñuelas and Staudt, 2010; Strada et al., 2023; Wang et al., 2022a). The winter levels remain relatively stable, as stored monoterpenes in plant tissues continue to be emitted even during periods of low biosynthesis (Bourtsoukidis et al., 2024; Ciccioli et al., 2023; Wang et al., 2022a, 2024). Consistent with the findings of Debevec et al., 2018, our observations also revealed elevated nighttime concentrations of monoterpenes, likely attributable to reduced oxidative sinks, boundary layer dynamics, and continuous emissions from vegetative storage pools.



405

Figure 4: Diurnal profiles (hourly averages) for mixing ratio (ppbv) of major VOCs. It includes terpenes(a-b), oxygenated VOCs (alcohols, carbonyls, acids, other oxygenated (c-k)), nitrogen and sulfur-containing VOCs (l-m), and aromatic hydrocarbons (n-p), measured at a rural background site in Cyprus from 2022 to 2024. Seasonal variations are color-coded, highlighting year-wise spring and summer trends alongside autumn, winter, and overall averages. Shaded areas indicate standard error for median values. X-axis here represents time in hours in UTC.



410 3.3.2 Oxygenated VOCs

Methanol and ethanol exhibited moderate diurnal variation with elevated daytime and evening levels in summer (Fig. 4c-d). Median methanol observed as $\sim 5.52 \pm 1.27$ ppbv and ethanol as $\sim 0.76 \pm 0.26$ ppbv in summer 2024, reflecting both biogenic emissions and anthropogenic activities such as solvent use and burning. Carbonyls including acetaldehyde (2.38 ± 1.21 ppbv) and acetone (415 3.82 ± 1.02 ppbv), displayed sharp midday peaks in summer, consistent with secondary formation via photochemical oxidation. Their diurnal and seasonal consistency between 2023 and 2024 highlights photochemical production pathways. Organic acids including formic and acetic acid showed significant daytime enhancements in summer, particularly in 2024. Their median mixing ratios reached 1.76 ± 0.70 ppbv and 5.60 ± 2.75 ppbv, respectively, suggesting combined direct (420 emissions and oxidative formation, possibly influenced by biomass burning or regional wildfires. Among other OVOCs, MVK, a product of isoprene oxidation, peaked at 0.15 ± 0.08 ppbv during summer midday. Furan, a tracer of biomass burning, showed morning maxima in summer 2023, indicating episodic fire activity. Consistent with isoprene emission, methyl vinyl ketone (MVK) also shows almost 42% of its emission during the summer season. A total of 60-70% levels of acetic (425 acid, acetaldehyde, acetone, formic acid, and methanol emissions occur during summer and spring season, collectively showing their biogenic dominance.

3.3.3 Nitrogen and sulfur-containing VOCs

Acetonitrile, a biomass burning tracer, showed minimal diurnal variation due to its long atmospheric lifetime, which is approximately 620 days (Robles, 2005). Nevertheless, elevated levels were (430 observed throughout the summer of 2023–2024, pointing to regional fire events or long-range transport. The median acetonitrile seasonal mixing ratios were found to be highest during summer 2024 as 0.17 ± 0.02 ppbv, while lowest during winter as 0.08 ± 0.01 ppbv. DMS average levels were observed highest during summer 2023 as 0.12 ± 0.09 ppbv, it could probably be due to enhanced marine biogenic emission from the nearby mediterranean sea. DMS strong seasonal signal supports (435 a temperature-driven biological origin (Deschaseaux et al., 2022; Edtbauer et al., 2020).

3.3.4 Aromatic hydrocarbons

Benzene showed summer midday enhancements (0.26 ± 0.12 ppbv), while toluene and xylene exhibited flatter or bimodal patterns (high during morning and evening, probably due to increased vehicular activities) with higher variability. Xylene and toluene mixing ratios peaked in winter and (440 spring, consistent with local combustion under shallow boundary layers. The large standard error variation (Fig. 4o-p), especially for xylene and toluene, indicates episodic anthropogenic inputs from traffic or regional pollution. Compared with benzene, these more reactive aromatics exhibited flat or noisy diurnal profiles with limited seasonal variability, aside from the winter-spring xylene enhancement.



445 3.4. Temperature-driven enhancement of VOC emissions in the eastern mediterranean

3.4.1. Temperature sensitivity of VOCs

The variation in VOC mixing ratios with temperature revealed clear temperature-dependent trends across most VOCs (Fig. 5). BVOCs, particularly isoprene, showed strong responses to rising temperatures, as their mixing ratio increased markedly beyond 25 °C, with a peak observed between
450 35–38 °C (0.53 ± 0.22 ppbv). There is an exponential increase in isoprene levels up to 38 °C, however, a slight decline (0.02 – 0.06 ppbv) in its level above 38 °C suggests crossing a tipping point through inhibition under extreme heat stress conditions (Fortunati et al., 2008). Monoterpenes exhibited a comparatively low increase in mixing ratios with an increase in temperature, and its trend was more gradual. The moderate rise at 35–38 °C (from 0.34 to 0.41 ppbv, ~21% increase) supports a biogenic
455 contribution during summer, while the relatively stable levels across temperature bins may indicate sustained emissions throughout the day.

DMS levels also rose steadily with temperature, with maximum values observed between 35–38 °C (0.18 ± 0.13 ppbv). This trend is likely driven by enhanced microbial activity in the mediterranean sea (Edtbauer et al., 2020) and increased volatilization rates in warm, semi-arid, and coastal
460 conditions typical of the region (Edtbauer et al., 2020). OVOCs also exhibited strong temperature dependence. Acetone and methanol levels increased progressively, reflecting a combination of direct biogenic emissions and secondary formation via oxidation of precursor compounds (Huang et al., 2020; Liu et al., 2009; Mellouki et al., 2015; Wang et al., 2022b). Methanol levels rose sharply above 38 °C (~19% with mean value of 4.85 ± 0.91 ppbv), consistent with known biogenic sources
465 such as plant metabolism and microbial activity (Dorokhov et al., 2018). Methanol is also produced during forest fire events, so one more probable cause could be increased fire activity with average temperature beyond 38 °C (Paton-Walsh et al., 2008; Yokelson et al., 1999). Acetic acid and acetaldehyde showed particularly sharp increases above 35 °C, with acetic acid levels ~2.8 times higher beyond 38 °C (5.4 ± 2.9 ppbv) when compared with the levels at 35–38 °C. These patterns
470 indicate enhanced photochemical production and possible evaporation-driven emissions (Debevec et al., 2017; Xu et al., 2023; Yuan et al., 2024). The increase of OVOCs under warmer conditions (>38 °C) highlights their potentially significant role in SOA formation in the EMME region (Azmi and Sharma, 2023; Pennington et al., 2021).

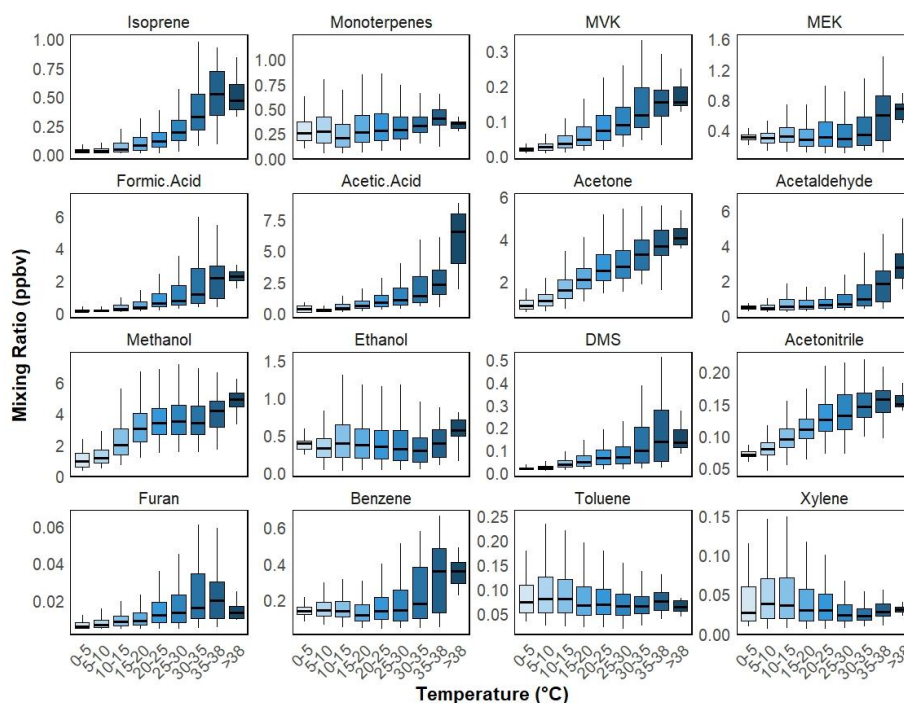
Among anthropogenic VOCs, benzene displayed a notable rise above 35 °C (0.35 ppbv), suggesting
475 contributions from evaporate emissions, or long-range transport (Dimitriou and Kassomenos, 2020; Gjesteland et al., 2019). Another possible reason for the high daytime benzene levels, particularly during hot days ($AT > 35^\circ\text{C}$) could be heat-stress-induced biogenic emissions (Miszta et al., 2015), where vegetation was found to release diverse benzenoid compounds under stress, potentially for communication or protective functions. However, the exact cause remains uncertain and warrants
480 further investigation. In contrast, both toluene and xylene levels were highest at lower temperatures (<15 °C), likely reflecting solvent use, decreased photochemistry, or indoor emissions during cooler periods (Abbasi et al., 2020; Song et al., 2011). A minor elevation (~0.01 ppbv) in toluene and



xylene was observed at 35–38 °C, potentially due to evaporative processes or reduced atmospheric dispersion.

485 3.4.2. Intensified VOC loading during the Summer 2024 heatwaves

490 June 2024 was the hottest month on record in Cyprus and coincided with the highest TVOCs mixing ratios observed during the 2022–2024 period (25.76 ± 8.29 ppbv), exceeding summer maxima recorded in 2023 and 2022 (Fig. S4). As illustrated in Fig. 4, most VOCs also showed markedly higher emissions in 2024 compared to previous years. Considering that our observations span only until 15 June 2024, we focused on the comparison of the first half of June across the three years. The data revealed that TVOCs mixing ratio in early June 2024 (23.53 ppbv) were more than double compared to those measured during the same period in 2022 (9.98 ppbv) and 2023 (8.59 ppbv). This sharp rise was accompanied by extreme meteorological conditions: record-breaking average temperatures (24.95 °C), intense SR (314.81 Wm^{-2}), and very low RH (27%). In contrast, temperatures in early June 2022 and 2023 averaged 21.91 °C and 20.61 °C, with RH at 59.73% and 56.39%, respectively.



500 **Figure 5: Temperature Dependence of Ambient VOC mixing ratio in Cyprus.** Box plots showing the variation in ambient mixing ratio (in ppbv) of selected VOCs across different temperature ranges (°C) at a rural background site in Cyprus. Each box represents the interquartile range (IQR) with the median marked, and whiskers indicating variability outside the upper and lower quartiles.

These conditions favored both primary BVOCs' emissions and secondary atmospheric processes. Rapid vegetative growth in spring, followed by early thermal stress, likely stimulated isoprene and



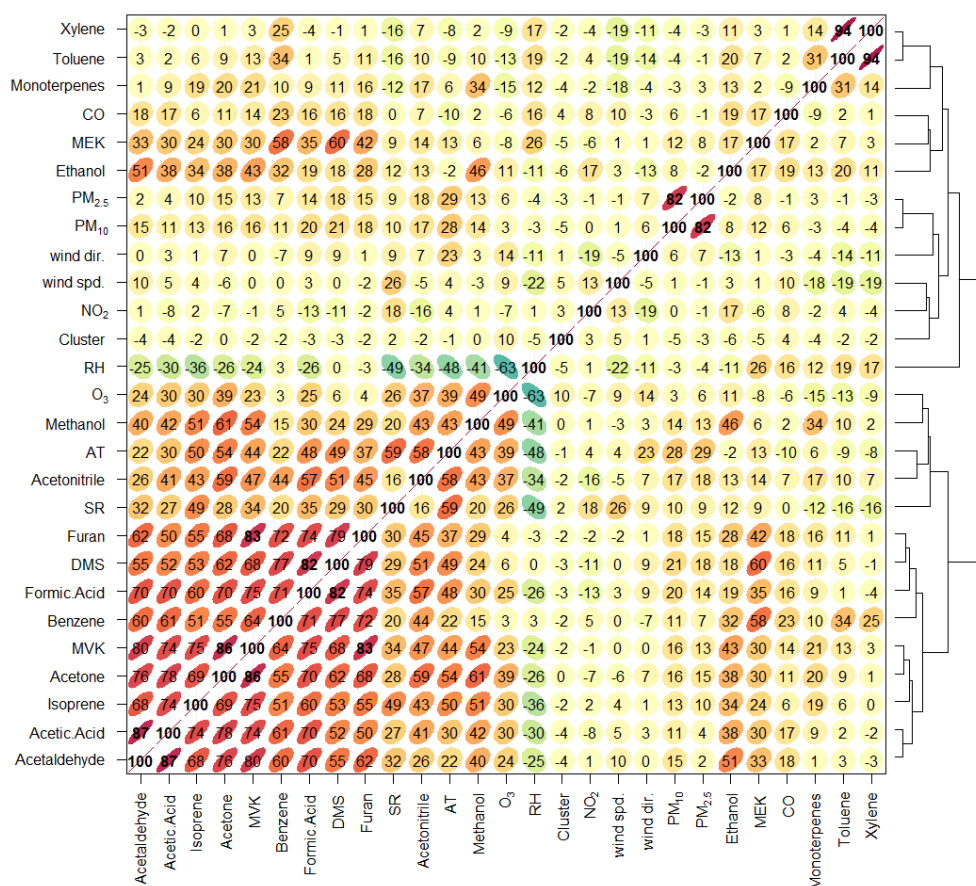
505 monoterpene emissions, and maybe also benzene. Elevated temperatures and oxidant availability enhanced both the emission (Bourtsoukidis et al., 2014) and formation of OVOCs such as acetaldehyde, acetic acid, and methanol. Concurrently, increased levels of CO (144.77 ppbv) and O₃ (58.77 ppbv) in 2024, compared to 2022 (132.69 and 45.13 ppbv) and 2023 (119.27 and 51.88 ppbv), indicate stronger photochemical activity and increased ozone formation potential.

510 Midday peaks in isoprene and monoterpenes, along with enhanced OVOCs mixing ratios (e.g., acetone, acetic acid, acetaldehyde), reflect intense photochemical production under elevated SR. Elevated MVK/isoprene ratio further confirm enhanced oxidation of biogenic precursors (Guo et al., 2012). The findings suggest that escalating heatwave intensity and frequency in the EMME region could significantly increase VOC burdens, contributing to secondary pollutant formation (O₃ and SOA) and worsening regional air quality.

515 3.5. Inter-species relationship

Based on the comprehensive correlation analysis in Fig. 6, clear patterns emerge among VOCs, meteorological parameters, and pollutant levels. The overall correlation matrix reveals strong positive associations among OVOCs such as acetaldehyde, acetic acid, ethanol, acetone, methanol, and formic acid, often with correlation coefficients $r > 0.6$ – 0.9 , suggesting common sources and atmospheric processes. Isoprene, monoterpenes, and MVK also correlate strongly, especially isoprene and MVK ($r = 0.75$), indicating secondary photochemical formation and biogenic influence during high radiation periods. Aromatic hydrocarbons (e.g., toluene and xylene) form another cluster with moderate-to-strong correlations ($r = 0.94$), consistent with urban combustion sources.

525 Seasonal correlation matrices (Fig. S6) highlight dynamic VOC-environment interactions. On the contrary, benzene-toluene ($r = 0.6$) and benzene-xylene ($r = 0.4$) correlation is moderate in winter, maybe due to low photochemical loss due to low temperature, but weakens in summer ($r < 0.3$) due to faster toluene degradation and variable sources (Gelencsér et al., 1997). In summer, BVOCs correlate most strongly with temperature and radiation, indicating dominant temperature-driven emissions. Winter shows weaker correlations due to reduced photochemistry and biogenic activity, while spring and autumn display moderate, transitional patterns. NO₂ and CO maintain consistent moderate correlations with aromatic VOCs (BTX) across seasons, underscoring persistent combustion and vehicular influences, either local or transported. RH shows negative correlations with most VOCs, likely due to emission suppression or enhanced wet removal. O₃ is positively correlated with reactive VOCs like isoprene and monoterpenes, reflecting active photochemical processes. WS and WD show weaker correlations but may still influence variability, as suggested by backward trajectory analysis in the section below. Overall hierarchical clustering in Fig. 6 groups of species by chemical and functional similarity. OVOCs cluster tightly, as do aromatics, while temperature, radiation, and ozone form a separate group. These clusters reflect common sources and atmospheric behaviors.



540

Figure 6: Correlation matrix and hierarchical clustering of VOCs, meteorological parameters, and air pollutants. Pearson correlation matrix illustrates the relationships among VOCs, meteorological variables (e.g., temperature, solar radiation, humidity), and air pollutants (NO₂, O₃, CO, PM_{2.5}, PM₁₀). Positive correlations are shown in orange to red, while negative correlations are represented in green to blue. Hierarchical clustering (dendrogram) on the right groups variables with similar correlation patterns. Strong intra-group correlations are observed among oxygenated VOCs (e.g., acetone, acetaldehyde, acetic acid), biogenic VOCs (e.g., isoprene, MVK, monoterpenes), and aromatic compounds (e.g., benzene, toluene, xylene), reflecting common emission sources and photochemical behavior.

545

550

The diurnal variation of selected interspecies mixing ratios (Fig. S7) reveals distinct patterns driven by emission sources, photochemical processing, and atmospheric reactivity. Ratios such as toluene/benzene, and xylene/benzene decrease during the day (minima: ~0.45, and ~0.15 respectively), indicating stronger photochemical degradation of toluene and xylene compared to the more stable benzene (Tiwari et al., 2010). The MVK/isoprene ratio increases from ~0.5 in the early morning to ~1.0 by midday, reflecting active daytime oxidation of isoprene to MVK (Guo et al., 2012). Similarly, the isoprene/monoterpenes ratio peaks around 1.2 between 10:00–14:00 UTC, highlighting the temperature- and radiation-driven nature of isoprene emissions, while monoterpenes remain relatively stable (Kienler-Scharr et al., 2009). The ozone/NO₂ ratio exhibits a strong daytime increase, rising from ~30 to over 60 at noon, reflecting photochemical ozone

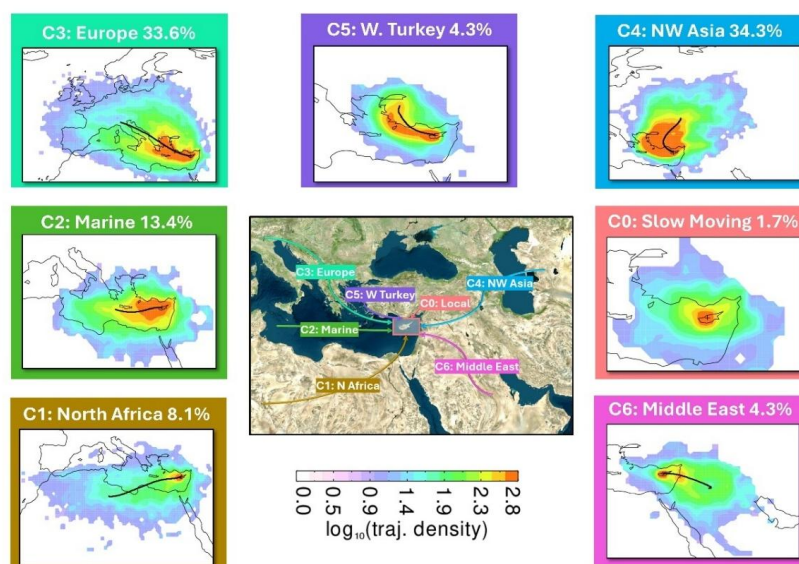
555



560 formation from NO₂ under solar radiation. Overall, the interspecies ratios effectively differentiate
between primary emissions and secondary formation, with photochemically active species
(isoprene, MVK, ozone) showing strong diurnal variability.

3.6. Air mass origins and transport patterns

565 Using the HYSPLIT model calculated air mass backward trajectories, we identified seven air mass
clusters (Fig. 7) that influences VOCs transport and composition over Cyprus. The dominant
clusters originated from Northwest Asia (C4, 34.3%) and Europe (C3, 33.6%), jointly accounting
for more than two-thirds of air mass transport. These clusters represent strong, recurrent long-range
transport from urbanized and industrialized continental regions and played a key role in shaping
seasonal and spatial VOC variability. Marine-influenced air masses (C2, 13.4%) reflected mixed
570 characteristics, carrying both marine biogenic signatures and aged anthropogenic pollution. Less
frequent clusters included air masses from North Africa (C1, 8.1%), Western Turkey (C5, 4.3%),
Middle East (C6, 4.3%), and stagnant local conditions (C0, 1.7%). Notably, C6, although infrequent
overall, was more prevalent during winter (10.7%) and exhibited elevated levels of benzene,
toluene, and xylene (BTX) during winter, suggesting long-range transport of AVOCs from the
575 Middle East. C0, characterized by low wind speeds and residence near the site, showed high
concentrations of primary pollutants such as benzene, acetonitrile, ethanol, and NO₂, consistent with
local anthropogenic and biomass burning sources.

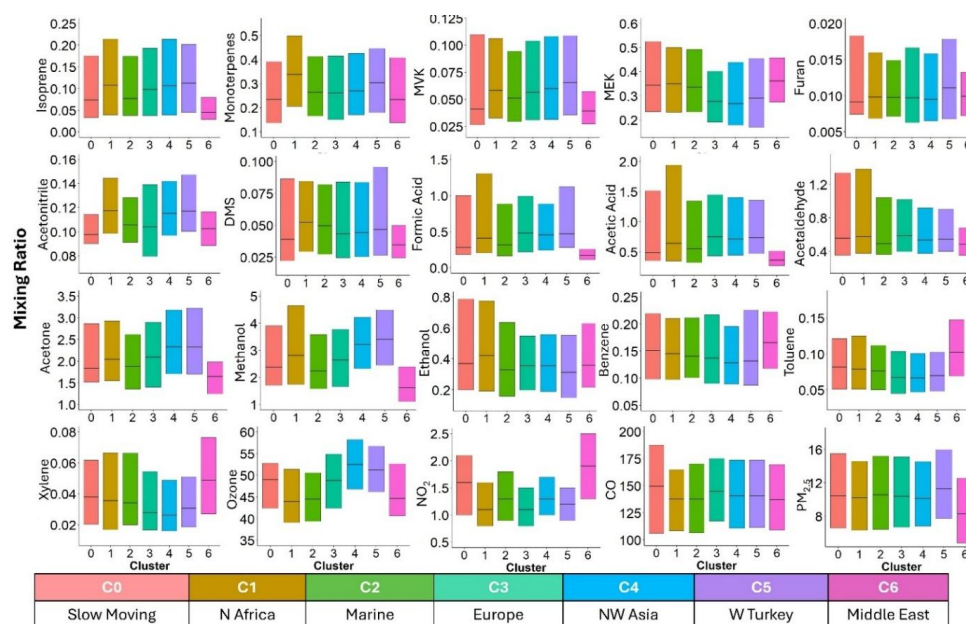


580 **Figure 7: Five-day air mass backward trajectories starting at 500 m above the ground level starting at every hour.** These were calculated from the NOAA ARL PC-version HYSPLIT transport and dispersion model using gridded wind fields from the GDAS, which has a spatial resolution of 1° × 1° longitude by latitude and a time resolution of 1 hr (Draxler and Hess, 1999) to demonstrate the influence of long-range transported air masses at the measurement site.



585 Distinct chemical signatures were observed across clusters. European clusters (C3) exhibited elevated OVOCs such as methanol, acetone, and acetic acid, indicating the presence of aged air masses and secondary formation processes. C3 also carried higher levels of isoprene and MVK, possibly from transported biogenic emissions. C4 was associated with elevated O₃, potentially due to photochemical aging during long-range transport. In contrast, Western Turkey (C5) air masses had generally low VOC mixing ratios, though slight O₃ enhancement was observed, possibly due to regional NO_x-rich emissions and transport.

590



595 **Figure 8: Mixing ratios of VOCs, and other air pollutants (in ppbv except PM_{2.5}, which is in µg m⁻³) across air mass clusters in the regional site at Eastern Mediterranean.** Boxplots showing the distribution of mixing ratios of selected VOCs, and other air pollutants for different air mass clusters (C0–C6) identified by back trajectory analysis. The black line within each box represents the median; boxes indicate the interquartile range, and whiskers denote variability outside the upper (75th) and lower (25th) quartiles.

600 Seasonal analysis (Fig. S8-S9) revealed pronounced variability in both air mass distribution and VOC loading. Spring and summer were dominated by clusters from Europe and NW Asia, corresponding with enhanced biogenic emissions, active photochemistry, and increased long-range transport. These seasons showed elevated mixing ratios of isoprene, monoterpenes, methanol, acetic acid, and O₃. Summer, and spring exhibited the highest overall VOC and O₃ levels across most clusters, underscoring strong atmospheric photochemical reactivity. Summer maintained high VOC loadings, particularly in C2 and C3 clusters, driven by elevated temperatures and insolation. Autumn displayed a relatively balanced air mass distribution with moderate VOC levels. Winter was characterized by reduced photochemical activity and lower overall VOC concentrations, except for C6, which exhibited persistently elevated anthropogenic markers such as BTX likely associated with heating-related emissions and regional transport under more stagnant meteorological conditions. These findings underscore the interplay between long-range transport, regional

605



610 meteorology, and local emissions in shaping atmospheric VOCs variability over Cyprus. The
combined influence of continental, marine, and regional sources contributes to complex
spatiotemporal variability, with implications for air quality, ozone formation, and atmospheric
oxidation capacity in the EMME region.

3.7. WRF-Chem model simulations

615 WRF-Chem simulations were evaluated against high-resolution PTR-ToF-MS observations
sampled at CAO-AMX across multiple seasons to assess the model's capability to reproduce VOCs
variability in the EMME region. BVOCs emissions were online estimated by MEGAN v2.1
(Guenther et al., 2012), while anthropogenic ones were based on EDGAR-HTAP for the outer
domains and a Cyprus high-resolution inventory for the innermost domain (Georgiou et al., 2020,
620 2022). Key biogenic species are isoprene and monoterpenes, while aromatics include benzene,
toluene, and xylene. These species, together with OVOCs, are evaluated using seasonal
distributions, diurnal behavior, and annual averages (Fig. 9, Figs. S10–S11).

Strong seasonal and daytime enhancements were found for terpenes, particularly during summer in
both observed and modelled mixing ratios due to temperature- and light-driven emissions. These
625 patterns are in good agreement with previous findings at other Mediterranean and European
background stations where biogenic fluxes are strongly modulated during periods of photochemical
activity (Ge et al., 2024; Genard-Zielinski et al., 2015). While the model captured the general
temporal dependence of isoprene ($r = 0.52$, $p < 0.05$), absolute mixing ratios were overestimated by
about a factor of 3. The study by Morichetti et al., 2022 observed that WRF-Chem simulations
630 using MEGAN v3.1 overpredicted isoprene emissions by approximately 20–40% across Europe,
particularly in southern regions. This bias was primarily attributed to the model's lack of an effective
drought stress response in the current MEGAN emission parameterization (Ge et al., 2024; Genard-
Zielinski et al., 2015; Morichetti et al., 2022). By contrast, Strada et al. (2023) reported strong
underprediction of isoprene mixing ratios for Cyprus, that was also attributed to water availability
635 dynamics, demonstrating inadequate understanding of the role of soil moisture in regulating
isoprene emissions in the EMME region.

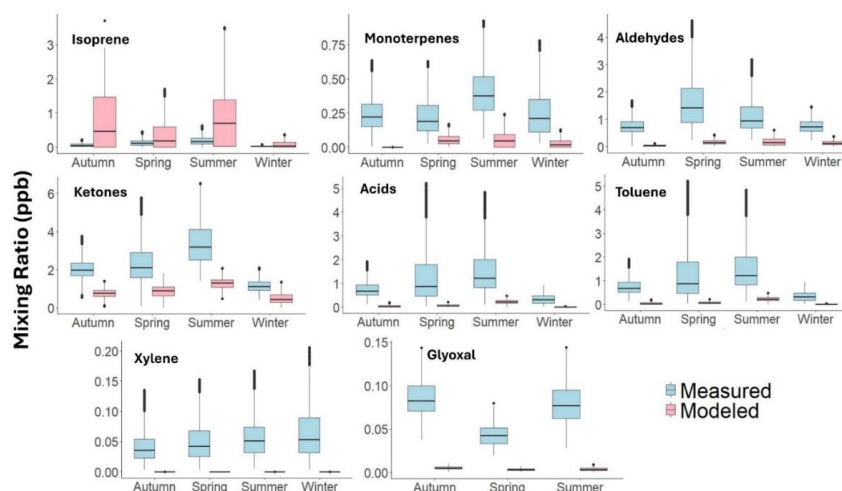
For monoterpenes, the model significantly underestimated the measured mixing ratios, by up to a
factor of 6-7 during the day and 3-4 at night (Fig. S11). The underestimation of monoterpenes in the
640 model could stem from the assumption that their emissions are primarily controlled by light and
temperature. If monoterpenes originate predominantly from storage pools, their fluxes will exhibit
only a weak light dependency, which could explain the observed discrepancies. In contrast, the
overestimation of isoprene in our study may be linked to heat- and drought-induced stress during
the summer months. Such conditions can alter plant carbon allocation strategies, leading to reduced
isoprene emissions and enhanced monoterpene release, consistent with observations reported by
645 (Byron et al., 2022).

OVOCs showed strong seasonal and diurnal enhancements in the observations, especially during
hot, dry summer periods with enhanced photochemical activity but were systematically and



650

consistently underestimated by the model. Mean mixing ratios of observed acids, aldehydes, and ketones were calculated 12, 9, and 3 times respectively higher than the model values. Similar discrepancies between observed and modeled OVOCs have been documented throughout Europe due to missing secondary formation chemistry, incomplete representation of oxidation products, and inadequate treatment of evaporative emissions during elevated temperatures (Ge et al., 2024). Taken together, these results indicate that there are significant deficiencies in the representation of OVOCs precursors and multi-phase processing by RACM.



655

Figure 9: Seasonal variation among measured and simulated VOCs mixing ratios at rural background site in Cyprus.

660

Aromatic VOCs like toluene and xylene showed relatively flat diurnal profiles with slight morning and evening peaks in cooler months (Fig. S11), indicative of local anthropogenic sources under stable atmospheric conditions. However, WRF-Chem significantly underestimated these species, particularly xylene, implying incomplete representation of urban emissions, traffic sources, and solvent use in anthropogenic inventories. Glyoxal, an important secondary oxidation product, exhibited a clear midday peak in measurements, but modeled values were significantly lower, even though the timing of the peak was captured, suggesting underestimation of precursor VOCs and low yields in photochemical pathways. Seasonal comparisons (Fig. 9) confirmed these discrepancies. Observed levels of isoprene, aldehydes, ketones, and monoterpenes peaked in spring and summer, consistent with enhanced biogenic and photochemical activity. Modeled outputs, however, underrepresented OVOCs and AVOCs across all seasons. Despite some agreement in seasonal patterns, WRF-Chem was unable to reproduce the magnitude and timing of peak VOC levels. The annual comparison (Fig. S10) showed that while isoprene mean simulated values were relatively aligned with observations, most other VOC groups, particularly OVOCs and aromatics, were systematically underestimated.

670

675

EDGAR generally reports higher VOC emissions compared to EMEP or CAMS-REG-AP due to differences in industrial combustion and fugitive sector representation (Thunis et al., 2021).



680 However, these differences in VOC emissions have a limited impact on European-scale ozone modelling, and chemical regime and meteorology remain dominant drivers of O₃ variability (Thunis et al., 2021). A high-resolution Cyprus inventory may significantly improve the spatial representation of anthropogenic emissions and reduces NO₂ and O₃ biases compared to simulations based on CAMS (Georgiou et al., 2022), but uncertainties in BVOCs and OVOCs sources remain the largest contributors to discrepancies.

685 Overall, the analysis reveals that the heat extremes of the Eastern Mediterranean evoke a distinctive VOC emission response that enhances differences between observations and models based on traditional parameterizations developed in temperate conditions. The systematic underprediction of monoterpenes and OVOCs, when taken together with the overestimation of isoprene, suggests that incorporation of drought-sensitive plant physiology, storage-driven emission dynamics, and extended secondary oxidation chemistry within regional air quality models is required. Both focused biogenic emission modeling efforts and OVOC reaction pathways are necessary to appropriately quantify atmospheric reactivity and chemical transport in this climate-sensitive region.

690 4 Conclusions

This study provides a comprehensive assessment of VOCs variability in the Eastern Mediterranean based on multi-year high-resolution PTR-ToF-MS observations at a rural background site in Cyprus, supported by meteorological data, HYSPLIT back trajectories, and WRF-Chem model simulations. VOCs were classified into biogenic, anthropogenic, and secondary/oxygenated types to enable interpretation under varying environmental conditions. OVOCs were the dominant chemical class, contributing approximately 79% to the total measured VOC burden.

700 BVOCs, particularly isoprene, exhibited pronounced summer peaks and daytime maxima, closely linked to solar radiation and temperature. Isoprene increased with temperature up to 38 °C before declining, suggesting thermal stress emission suppression, while monoterpenes showed both daytime and nocturnal presence may be due to diverse emission drivers from vegetation, boundary layer dynamics, or anthropogenic contribution. OVOCs (acetone, methanol, acetic acid, acetaldehyde) were enhanced during hot, dry periods, indicating amplified emission and photochemical formation. DMS peaks under high temperatures pointed to microbial activity and volatilization in semi-arid and coastal environments. Among AVOCs, benzene increased sharply above 35 °C, likely from evaporative emissions and long-range transport, whereas toluene and xylene were more abundant in cooler periods and degraded rapidly at higher temperatures.

705 HYSPLIT trajectory cluster analysis revealed elevated AVOCs, especially aromatics, under the influence of long-range transported continental air masses from Europe, NW Asia, the Middle East, and SW Asia. The variability in organic acid and sulfur compound was attributed to marine and North African air masses. Slow-moving local air masses, although infrequent, showed disproportionately high VOCs mixing ratio, indicating strong local emission influence. Seasonal patterns showed summer dominated by biogenic emissions and active photochemistry, while winter



was characterized by anthropogenic influences under stagnant conditions; spring emerged as a particularly reactive period.

715 WRF-Chem model simulations captured general seasonal patterns of biogenic isoprene but systematically underpredicted OVOCs, aromatics, and secondary VOCs, with notable temporal mismatches in diurnal cycles. These shortcomings reflect limitations in emission inventories, oxidation schemes, and meteorological coupling, particularly for region-specific and stress-induced emissions.

720 Overall, VOC variability over Cyprus is driven by the interplay of heat, seasonality, source type, meteorology, and long-range transport. The findings underscore the need for improved VOC parameterizations in regional to global models, region-specific source inventories, and adaptive air quality management strategies that account for both local and long-range transported emissions. A dedicated source apportionment analysis would be a valuable follow-up to this work, allowing for
725 quantitative attribution of the observed VOCs to specific sources. With projected increases in climatic extremes in the EMME region, understanding these processes is critical for improved tropospheric ozone budget, secondary organic aerosol production, and broader air quality and climate impacts.

730 **Data availability.** All data used in this study are openly available at <https://zenodo.org/records/17483541>

Author Contribution.

AG: Conceptualization, Data curation, Methodology, Validation, Formal analysis, Investigation, Writing – original draft, Writing – review & editing, Visualization. MD: Data curation,
735 Methodology, Software, Validation, Formal analysis, Writing – review & editing. AC: Methodology, Data curation, Formal analysis, Writing – review & editing. TC: Data curation, Software, Writing – review & editing. VPK: Methodology, Software, Writing – review & editing. CS: Data curation, Resources, Writing – review & editing. MV: Methodology, Writing – review & editing. SN: Formal
740 analysis, Writing – review & editing. TJ: Writing – review & editing. JB: Writing – review & editing. JW: Writing – review & editing. NM: Writing – review & editing. EL: Writing – review & editing. JS: Funding acquisition, Resources, Writing – review & editing. EB: Conceptualization, Project administrator, Methodology, Validation, Investigation, Writing – review & editing, Supervision.

Competing interests.

The contact author has declared that none of the authors has any competing interests.



745 **Acknowledgements.**

This work was supported by the European Union's Horizon 2020 research and innovation program (grant No. 856612) and the Cyprus Government (EMME-CARE). The authors thank the CAO technical team for the routine upkeep of the AMX station. EB and SN acknowledge support from the project EVOCPOLIS funded by The Cyprus Research and Innovation Foundation (RIF), implemented under the Cohesion Policy Programme “Thalia 2021-2027” and co-funded by the EU. TJ and VPK are supported by the European Union ERC-2022-STGERC-BAE-Project: 101076311. Views and opinions expressed are however those of the author(s) only and do not necessarily reflect those of the European Union or the European Research Council Executive Agency. Neither the European Union nor the granting authority can be held responsible for them.

755 **References**

- Abbasi, F., Pasalari, H., Delgado-Saborit, J. M., Rafiee, A., Abbasi, A., and Hoseini, M.: Characterization and risk assessment of BTEX in ambient air of a Middle Eastern City, *Process Safety and Environmental Protection*, 139, 98–105, <https://doi.org/10.1016/j.psep.2020.03.019>, 2020.
- Atkinson, R.: Atmospheric chemistry of VOCs and NO_x, *Atmos Environ*, 34, 2063–2101, [https://doi.org/10.1016/S1352-2310\(99\)00460-4](https://doi.org/10.1016/S1352-2310(99)00460-4), 2000.
- Azmi, S. and Sharma, M.: Global PM_{2.5} and secondary organic aerosols (SOA) levels with sectorial contribution to anthropogenic and biogenic SOA formation, *Chemosphere*, 336, <https://doi.org/10.1016/j.chemosphere.2023.139195>, 2023.
- 760 Baalbaki, R., Pikridas, M., Jokinen, T., Laurila, T., Dada, L., Bezantakos, S., Ahonen, L., Neitola, K., Maissner, A., Bimenyimana, E., Christodoulou, A., Unga, F., Savvides, C., Lehtipalo, K., Kangasluoma, J., Biskos, G., Petäjä, T., Kerminen, V.-M., Sciare, J., and Kulmala, M.: Towards understanding the characteristics of new particle formation in the Eastern Mediterranean, *Atmos Chem Phys*, 21, 9223–9251, <https://doi.org/10.5194/acp-21-9223-2021>, 2021.
- 770 Boursoukidis, E., Williams, J., Kesselmeier, J., Jacobi, S., and Bonn, B.: From emissions to ambient mixing ratios: online seasonal field measurements of volatile organic compounds over a Norway spruce-dominated forest in central Germany, *Atmos Chem Phys*, 14, 6495–6510, <https://doi.org/10.5194/acp-14-6495-2014>, 2014.
- 775 Boursoukidis, E., Behrendt, T., Yañez-Serrano, A. M., Hellén, H., Diamantopoulos, E., Catão, E., Ashworth, K., Pozzer, A., Quesada, C. A., Martins, D. L., Sá, M., Araujo, A., Brito, J., Artaxo, P., Kesselmeier, J., Lelieveld, J., and Williams, J.: Strong sesquiterpene emissions from Amazonian soils, *Nat Commun*, 9, 2226, <https://doi.org/10.1038/s41467-018-04658-y>, 2018.
- Boursoukidis, E., Ernle, L., Crowley, J. N., Lelieveld, J., Paris, J.-D., Pozzer, A., Walter, D., and Williams, J.: Non-methane hydrocarbon (C₂–C₈) sources and sinks around the Arabian Peninsula, *Atmos Chem Phys*, 19, 7209–7232, <https://doi.org/10.5194/acp-19-7209-2019>, 2019.
- 780 Boursoukidis, E., Pozzer, A., Williams, J., Makowski, D., Peñuelas, J., Matthaios, V. N., Lazoglou, G., Yañez-Serrano, A. M., Lelieveld, J., Ciais, P., Vrekoussis, M., Daskalakis, N., and Sciare, J.: High temperature sensitivity of monoterpene emissions from global vegetation, *Commun Earth Environ*, 5, 23, <https://doi.org/10.1038/s43247-023-01175-9>, 2024.
- 785 Boursoukidis, E., Guenther, A., Wang, H., Economou, T., Lazoglou, G., Christodoulou, A., Christoudias, T., Nölscher, A., Yañez-Serrano, A. M., and Peñuelas, J.: Environmental Change Is



- Reshaping the Temperature Sensitivity of Sesquiterpene Emissions and Their Atmospheric Impacts, *Glob Chang Biol*, 31, <https://doi.org/10.1111/gcb.70258>, 2025.
- 790 Brito, J., Freney, E., Dominutti, P., Borbon, A., Haslett, S. L., Batenburg, A. M., Colomb, A., Dupuy, R., Denjean, C., Burnet, F., Bourriane, T., Deroubaix, A., Sellegri, K., Borrmann, S., Coe, H., Flamant, C., Knippertz, P., and Schwarzenboeck, A.: Assessing the role of anthropogenic and biogenic sources on PM_{2.5} over southern West Africa using aircraft measurements, *Atmos Chem Phys*, 18, 757–772, <https://doi.org/10.5194/acp-18-757-2018>, 2018.
- 795 Byron, J., Kreuzwieser, J., Purser, G., van Haren, J., Ladd, S. N., Meredith, L. K., Werner, C., and Williams, J.: Chiral monoterpenes reveal forest emission mechanisms and drought responses, *Nature*, 609, 307–312, <https://doi.org/10.1038/s41586-022-05020-5>, 2022.
- 800 Capes, G., Murphy, J. G., Reeves, C. E., Mcquaid, J. B., Hamilton, J. F., Hopkins, J. R., Crosier, J., Williams, P. I., and Coe, H.: Secondary organic aerosol from biogenic VOCs over West Africa during AMMA, *Atmos. Chem. Phys.*, 3841–3850 pp., 2009.
- 805 Ciccio, P., Silibello, C., Finardi, S., Pepe, N., Ciccio, P., Rapparini, F., Neri, L., Fares, S., Brilli, F., Mircea, M., Magliulo, E., and Baraldi, R.: The potential impact of biogenic volatile organic compounds (BVOCs) from terrestrial vegetation on a Mediterranean area using two different emission models, *Agric For Meteorol*, 328, 109255, <https://doi.org/10.1016/j.agrformet.2022.109255>, 2023.
- 810 Civan, M. Y., Elbir, T., Seyfioglu, R., Kuntasal, Ö. O., Bayram, A., Doğan, G., Yurdakul, S., Andıç, Ö., Müezzinoğlu, A., Sofuoğlu, S. C., Pekey, H., Pekey, B., Bozlaker, A., Odabasi, M., and Tuncel, G.: Spatial and temporal variations in atmospheric VOCs, NO₂, SO₂, and O₃ concentrations at a heavily industrialized region in Western Turkey, and assessment of the carcinogenic risk levels of benzene, *Atmos Environ*, 103, 102–113, <https://doi.org/10.1016/j.atmosenv.2014.12.031>, 2015.
- Cyprus Mail: Last month hottest June ever in Cyprus., *Cyprus Mail*, 2024.
- 815 Das, A., Giri, B. S., and Manjunatha, R.: Systematic review on benzene, toluene, ethylbenzene, and xylene (BTEX) emissions; health impact assessment; and detection techniques in oil and natural gas operations, *Environmental Science and Pollution Research*, 32, 1–22, <https://doi.org/10.1007/s11356-024-35698-1>, 2024.
- 820 Debevec, C., Sauvage, S., Gros, V., Sciare, J., Pikridas, M., Stavroulas, I., Salameh, T., Leonardis, T., Gaudion, V., Depelchin, L., Fronval, I., Sarda-Esteve, R., Baisnée, D., Bonsang, B., Savvides, C., Vrekoussis, M., and Locoge, N.: Origin and variability in volatile organic compounds observed at an Eastern Mediterranean background site (Cyprus), *Atmos Chem Phys*, 17, 11355–11388, <https://doi.org/10.5194/acp-17-11355-2017>, 2017.
- 825 Debevec, C., Sauvage, S., Gros, V., Sellegri, K., Sciare, J., Pikridas, M., Stavroulas, I., Leonardis, T., Gaudion, V., Depelchin, L., Fronval, I., Sarda-Esteve, R., Baisnée, D., Bonsang, B., Savvides, C., Vrekoussis, M., and Locoge, N.: Driving parameters of biogenic volatile organic compounds and consequences on new particle formation observed at an eastern Mediterranean background site, *Atmos Chem Phys*, 18, 14297–14325, <https://doi.org/10.5194/acp-18-14297-2018>, 2018.
- 830 Derstroff, B., Hüser, I., Bourtsoukidis, E., Crowley, J. N., Fischer, H., Gromov, S., Harder, H., Janssen, R. H. H., Kesselmeier, J., Lelieveld, J., Mallik, C., Martinez, M., Novelli, A., Parchatka, U., Phillips, G. J., Sander, R., Sauvage, C., Schuladen, J., Stönnner, C., Tomsche, L., and Williams, J.: Volatile organic compounds (VOCs) in photochemically aged air from the eastern and western Mediterranean, *Atmos Chem Phys*, 17, 9547–9566, <https://doi.org/10.5194/acp-17-9547-2017>, 2017.



- 835 Deschaseaux, E. S. M., Swan, H. B., Maher, D. T., Jones, G. B., Schulz, K. G., Koveke, E. P., Toda, K., and Eyre, B. D.: The Interplay Between Dimethyl Sulfide (DMS) and Methane (CH₄) in a Coral Reef Ecosystem, *Front Mar Sci*, 9, <https://doi.org/10.3389/fmars.2022.910441>, 2022.
- Desservettaz, M., Pikridas, M., Stavroulas, I., Bougiatioti, A., Liakakou, E., Hatzianastassiou, N., Sciare, J., Mihalopoulos, N., and Bourtsoukidis, E.: Emission of volatile organic compounds from residential biomass burning and their rapid chemical transformations, *Science of The Total Environment*, 903, 166592, <https://doi.org/10.1016/j.scitotenv.2023.166592>, 2023.
- 840 Dimitriou, K. and Kassomenos, P.: Background concentrations of benzene, potential long range transport influences and corresponding cancer risk in four cities of central Europe, in relation to air mass origination, *J Environ Manage*, 262, 110374, <https://doi.org/10.1016/j.jenvman.2020.110374>, 2020.
- 845 Dorokhov, Y. L., Sheshukova, E. V., and Komarova, T. V.: Methanol in Plant Life, *Front Plant Sci*, 9, <https://doi.org/10.3389/fpls.2018.01623>, 2018.
- Draxler, R. R. and H. G. D.: Description of the HYSPLIT_4 modeling system., Silver Spring, 24 pp., 1997.
- 850 Edtbauer, A., Stöner, C., Pfannerstill, E. Y., Berasategui, M., Walter, D., Crowley, J. N., Lelieveld, J., and Williams, J.: A new marine biogenic emission: methane sulfonamide (MSAM), dimethyl sulfide (DMS), and dimethyl sulfone (DMSO₂) measured in air over the Arabian Sea, *Atmos Chem Phys*, 20, 6081–6094, <https://doi.org/10.5194/acp-20-6081-2020>, 2020.
- 855 Ehn, M., Thornton, J. A., Kleist, E., Sipilä, M., Junninen, H., Pullinen, I., Springer, M., Rubach, F., Tillmann, R., Lee, B., Lopez-Hilfiker, F., Andres, S., Acir, I.-H., Rissanen, M., Jokinen, T., Schobesberger, S., Kangasluoma, J., Kontkanen, J., Nieminen, T., Kurtén, T., Nielsen, L. B., Jørgensen, S., Kjaergaard, H. G., Canagaratna, M., Maso, M. D., Berndt, T., Petäjä, T., Wahner, A., Kerminen, V.-M., Kulmala, M., Worsnop, D. R., Wildt, J., and Mentel, T. F.: A large source of low-volatility secondary organic aerosol, *Nature*, 506, 476–479, <https://doi.org/10.1038/nature13032>, 2014.
- 860 Emekwuru, N. and Ejohwomu, O.: Temperature, Humidity and Air Pollution Relationships during a Period of Rainy and Dry Seasons in Lagos, West Africa, *Climate*, 11, 113, <https://doi.org/10.3390/cli11050113>, 2023.
- 865 Fortunati, A., Barta, C., Brilli, F., Centritto, M., Zimmer, I., Schnitzler, J., and Loreto, F.: Isoprene emission is not temperature-dependent during and after severe drought-stress: a physiological and biochemical analysis, *The Plant Journal*, 55, 687–697, <https://doi.org/10.1111/j.1365-313X.2008.03538.x>, 2008.
- Gelencsér, A., Siszler, K., and Hlavay, J.: Toluene–Benzene Concentration Ratio as a Tool for Characterizing the Distance from Vehicular Emission Sources, *Environ Sci Technol*, 31, 2869–2872, <https://doi.org/10.1021/es970004c>, 1997.
- 870 Georgiou, G. K., Kushta, J., Christoudias, T., Proestos, Y., and Lelieveld, J.: Air quality modelling over the Eastern Mediterranean: Seasonal sensitivity to anthropogenic emissions, *Atmos Environ*, 222, 117119, <https://doi.org/10.1016/j.atmosenv.2019.117119>, 2020.
- 875 Georgiou, G. K., Christoudias, T., Proestos, Y., Kushta, J., Pikridas, M., Sciare, J., Savvides, C., and Lelieveld, J.: Evaluation of WRF-Chem model (v3.9.1.1) real-time air quality forecasts over the Eastern Mediterranean, *Geosci Model Dev*, 15, 4129–4146, <https://doi.org/10.5194/gmd-15-4129-2022>, 2022.
- Germain-Piaulenne, E., Paris, J.-D., Gros, V., Quéhé, P.-Y., Pikridas, M., Baisnée, D., Berchet, A., Sciare, J., and Bourtsoukidis, E.: Middle East oil and gas methane emissions signature captured at



- a remote site using light hydrocarbon tracers, *Atmos Environ X*, 22, 100253, <https://doi.org/10.1016/j.aeaoa.2024.100253>, 2024.
- 880 Gjesteland, I., Hollund, B. E., Kirkeleit, J., Daling, P. S., Sørheim, K. R., and Bråtveit, M.: Determinants of airborne benzene evaporating from fresh crude oils released into seawater, *Mar Pollut Bull*, 140, 395–402, <https://doi.org/10.1016/j.marpolbul.2018.12.045>, 2019.
- Gu, S., Guenther, A., and Faiola, C.: Effects of Anthropogenic and Biogenic Volatile Organic Compounds on Los Angeles Air Quality, *Environ Sci Technol*, 55, 12191–12201, <https://doi.org/10.1021/acs.est.1c01481>, 2021.
- 885 Guo, H., Ling, Z. H., Simpson, I. J., Blake, D. R., and Wang, D. W.: Observations of isoprene, methacrolein (MAC) and methyl vinyl ketone (MVK) at a mountain site in Hong Kong, *Journal of Geophysical Research: Atmospheres*, 117, <https://doi.org/10.1029/2012JD017750>, 2012.
- Holzinger, R., Williams, J., Salisbury, G., Klüpfel, T., de Reus, M., Traub, M., Crutzen, P. J., and Lelieveld, J.: Oxygenated compounds in aged biomass burning plumes over the Eastern Mediterranean: evidence for strong secondary production of methanol and acetone, *Atmos Chem Phys*, 5, 39–46, <https://doi.org/10.5194/acp-5-39-2005>, 2005.
- 890 Huang, X.-F., Zhang, B., Xia, S.-Y., Han, Y., Wang, C., Yu, G.-H., and Feng, N.: Sources of oxygenated volatile organic compounds (OVOCs) in urban atmospheres in North and South China, *Environmental Pollution*, 261, 114152, <https://doi.org/10.1016/j.envpol.2020.114152>, 2020.
- Huangfu, Y., Yuan, B., Wang, S., Wu, C., He, X., Qi, J., de Gouw, J., Warneke, C., Gilman, J. B., Wisthaler, A., Karl, T., Graus, M., Jobson, B. T., and Shao, M.: Revisiting Acetonitrile as Tracer of Biomass Burning in Anthropogenic-Influenced Environments, *Geophys Res Lett*, 48, <https://doi.org/10.1029/2020GL092322>, 2021.
- 900 Kajos, M. K., Rantala, P., Hill, M., Hellén, H., Aalto, J., Patokoski, J., Taipale, R., Hoerger, C. C., Reimann, S., Ruuskanen, T. M., Rinne, J., and Petäjä, T.: Ambient measurements of aromatic and oxidized VOCs by PTR-MS and GC-MS: intercomparison between four instruments in a boreal forest in Finland, *Atmos Meas Tech*, 8, 4453–4473, <https://doi.org/10.5194/amt-8-4453-2015>, 2015.
- 905 Kaltsonoudis, C., Kostenidou, E., Florou, K., Psychoudaki, M., and Pandis, S. N.: Temporal variability and sources of VOCs in urban areas of the eastern Mediterranean, *Atmos Chem Phys*, 16, 14825–14842, <https://doi.org/10.5194/acp-16-14825-2016>, 2016.
- Kamal, M. S., Razzak, S. A., and Hossain, M. M.: Catalytic oxidation of volatile organic compounds (VOCs) – A review, *Atmos Environ*, 140, 117–134, <https://doi.org/10.1016/j.atmosenv.2016.05.031>, 2016.
- 910 Kiendler-Scharr, A., Wildt, J., Maso, M. D., Hohaus, T., Kleist, E., Mentel, T. F., Tillmann, R., Uerlings, R., Schurr, U., and Wahner, A.: New particle formation in forests inhibited by isoprene emissions, *Nature*, 461, 381–384, <https://doi.org/10.1038/nature08292>, 2009.
- 915 Kleanthous, S., Vrekoussis, M., Mihalopoulos, N., Kalabokas, P., and Lelieveld, J.: On the temporal and spatial variation of ozone in Cyprus, *Science of The Total Environment*, 476–477, 677–687, <https://doi.org/10.1016/j.scitotenv.2013.12.101>, 2014.
- Koppmann, R.: Chemistry of Volatile Organic Compounds in the Atmosphere, in: *Hydrocarbons, Oils and Lipids: Diversity, Origin, Chemistry and Fate*, Springer International Publishing, Cham, 811–822, https://doi.org/10.1007/978-3-319-90569-3_24, 2020.
- 920



- Koppmann, R., von Czapiewski, K., and Reid, J. S.: A review of biomass burning emissions, part I: gaseous emissions of carbon monoxide, methane, volatile organic compounds, and nitrogen containing compounds, <https://doi.org/10.5194/acpd-5-10455-2005>, 24 October 2005.
- 925 Lazoglou, G., Hadjinicolaou, P., Sofokleous, I., Bruggeman, A., and Zittis, G.: Climate change and extremes in the Mediterranean island of Cyprus: from historical trends to future projections, *Environ Res Commun*, 6, 095020, <https://doi.org/10.1088/2515-7620/ad7927>, 2024.
- Lee, J. D., Squires, F. A., Sherwen, T., Wilde, S. E., Cliff, S. J., Carpenter, L. J., Hopkins, J. R., Bauguutte, S. J., Reed, C., Barker, P., Allen, G., Bannan, T. J., Matthews, E., Mehra, A., Percival, C., Heard, D. E., Whalley, L. K., Ronnie, G. V., Seldon, S., Ingham, T., Keller, C. A., Knowland, K. E., Nisbet, E. G., and Andrews, S.: Ozone production and precursor emission from wildfires in Africa, *Environmental Science: Atmospheres*, 1, 524–542, <https://doi.org/10.1039/D1EA00041A>, 2021.
- 930
- Lelieveld, J., Berresheim, H., Borrmann, S., Crutzen, P. J., Dentener, F. J., Fischer, H., Feichter, J., Flatau, P. J., Heland, J., Holzinger, R., Korrmann, R., Lawrence, M. G., Levin, Z., Markowicz, K. M., Mihalopoulos, N., Minikin, A., Ramanathan, V., de Reus, M., Roelofs, G. J., Scheeren, H. A., Sciare, J., Schlager, H., Schultz, M., Siegmund, P., Steil, B., Stephanou, E. G., Stier, P., Traub, M., Warneke, C., Williams, J., and Ziereis, H.: Global Air Pollution Crossroads over the Mediterranean, *Science* (1979), 298, 794–799, <https://doi.org/10.1126/science.1075457>, 2002.
- 935
- Liakakou, E., Vrekoussis, M., Bonsang, B., Donousis, Ch., Kanakidou, M., and Mihalopoulos, N.: Isoprene above the Eastern Mediterranean: Seasonal variation and contribution to the oxidation capacity of the atmosphere, *Atmos Environ*, 41, 1002–1010, <https://doi.org/10.1016/j.atmosenv.2006.09.034>, 2007.
- 940
- Liakakou, E., Bonsang, B., Williams, J., Kalivitis, N., Kanakidou, M., and Mihalopoulos, N.: C2–C8 NMHCs over the Eastern Mediterranean: Seasonal variation and impact on regional oxidation chemistry, *Atmos Environ*, 43, 5611–5621, <https://doi.org/10.1016/j.atmosenv.2009.07.067>, 2009.
- 945
- Liu, Y., Shao, M., Kuster, W. C., Goldan, P. D., Li, X., Lu, S., and Gouw, J. A. de: Source Identification of Reactive Hydrocarbons and Oxygenated VOCs in the Summertime in Beijing, *Environ Sci Technol*, 43, 75–81, <https://doi.org/10.1021/es801716n>, 2009.
- 950
- Matthew, O. J.: Estimation of diurnal patterns of global solar radiation, temperature, relative humidity and wind speed from daily datasets at a humid tropical location, *Agric For Meteorol*, 322, 109003, <https://doi.org/10.1016/j.agrformet.2022.109003>, 2022.
- Mecca, M., Todaro, L., D’Auria, M., Italiano, S. S. P., Sofo, A., and Ripullone, F.: Volatile Organic Compounds (VOCs) in Mediterranean Oak Forests of Hungarian Oak (*Quercus frainetto* Ten) Affected by Dieback Phenomena, *Forests*, 15, 1072, <https://doi.org/10.3390/f15061072>, 2024.
- 955
- Mellouki, A., Wallington, T. J., and Chen, J.: Atmospheric Chemistry of Oxygenated Volatile Organic Compounds: Impacts on Air Quality and Climate, *Chem Rev*, 115, 3984–4014, <https://doi.org/10.1021/cr500549n>, 2015.
- 960
- Misztal, P. K., Hewitt, C. N., Wildt, J., Blande, J. D., Eller, A. S. D., Fares, S., Gentner, D. R., Gilman, J. B., Graus, M., Greenberg, J., Guenther, A. B., Hansel, A., Harley, P., Huang, M., Jardine, K., Karl, T., Kaser, L., Keutsch, F. N., Kiendler-Scharr, A., Kleist, E., Lerner, B. M., Li, T., Mak, J., Nölscher, A. C., Schnitzhofer, R., Sinha, V., Thornton, B., Warneke, C., Wegener, F., Werner, C., Williams, J., Worton, D. R., Yassaa, N., and Goldstein, A. H.: Atmospheric benzenoid emissions from plants rival those from fossil fuels, *Sci Rep*, 5, 12064, <https://doi.org/10.1038/srep12064>, 2015.
- 965
- Monson, R. K., Jaeger, C. H., Adams, W. W., Driggers, E. M., Silver, G. M., and Fall, R.: Relationships among Isoprene Emission Rate, Photosynthesis, and Isoprene Synthase Activity as



- Influenced by Temperature, *Plant Physiol*, 98, 1175–1180, <https://doi.org/10.1104/pp.98.3.1175>, 1992.
- 970 Mukherjee, S., Pandithurai, G., Waghmare, V., Mahajan, A. S., Tinel, L., Aslam, M. Y., Meena, G. S., Patil, S., Buchunde, P., and Kumar, A.: Seasonal variability of volatile organic compounds (VOCs) at a high-altitude station in the Western Ghats, India: Influence of biogenic, anthropogenic emissions and long-range transport, *Atmos Environ*, 331, 120598, <https://doi.org/10.1016/j.atmosenv.2024.120598>, 2024.
- 975 Pagonis, D., Sekimoto, K., and de Gouw, J.: A Library of Proton-Transfer Reactions of H_3O^+ Ions Used for Trace Gas Detection, *J Am Soc Mass Spectrom*, 30, 1330–1335, <https://doi.org/10.1007/s13361-019-02209-3>, 2019.
- 980 Panopoulou, A., Liakakou, E., Gros, V., Sauvage, S., Locoge, N., Bonsang, B., Psiloglou, B. E., Gerasopoulos, E., and Mihalopoulos, N.: Non-methane hydrocarbon variability in Athens during wintertime: the role of traffic and heating, *Atmos Chem Phys*, 18, 16139–16154, <https://doi.org/10.5194/acp-18-16139-2018>, 2018.
- Panopoulou, A., Liakakou, E., Sauvage, S., Gros, V., Locoge, N., Stavroulas, I., Bonsang, B., Gerasopoulos, E., and Mihalopoulos, N.: Yearlong measurements of monoterpenes and isoprene in a Mediterranean city (Athens): Natural vs anthropogenic origin, *Atmos Environ*, 243, 117803, <https://doi.org/10.1016/j.atmosenv.2020.117803>, 2020.
- 985 Paton-Walsh, C., Wilson, S. R., Jones, N. B., and Griffith, D. W. T.: Measurement of methanol emissions from Australian wildfires by ground-based solar Fourier transform spectroscopy, *Geophys Res Lett*, 35, <https://doi.org/10.1029/2007GL032951>, 2008.
- 990 Pennington, E. A., Seltzer, K. M., Murphy, B. N., Qin, M., Seinfeld, J. H., and Pye, H. O. T.: Modeling secondary organic aerosol formation from volatile chemical products, *Atmos Chem Phys*, 21, 18247–18261, <https://doi.org/10.5194/acp-21-18247-2021>, 2021.
- Peñuelas, J. and Staudt, M.: BVOCs and global change, *Trends Plant Sci*, 15, 133–144, <https://doi.org/10.1016/j.tplants.2009.12.005>, 2010.
- 995 Pérez, I. A., García, M. Á., Sánchez, M. L., Pardo, N., and Fernández-Duque, B.: Key Points in Air Pollution Meteorology, *Int J Environ Res Public Health*, 17, 8349, <https://doi.org/10.3390/ijerph17228349>, 2020.
- Perrone, M. G., Carbone, C., Faedo, D., Ferrero, L., Maggioni, A., Sangiorgi, G., and Bolzacchini, E.: Exhaust emissions of polycyclic aromatic hydrocarbons, n-alkanes and phenols from vehicles coming within different European classes, *Atmos Environ*, 82, 391–400, <https://doi.org/10.1016/j.atmosenv.2013.10.040>, 2014.
- 1000 Pikridas, M., Vrekoussis, M., Sciare, J., Kleanthous, S., Vasiliadou, E., Kizas, C., Savvides, C., and Mihalopoulos, N.: Spatial and temporal (short and long-term) variability of submicron, fine and sub-10 μm particulate matter (PM₁, PM_{2.5}, PM₁₀) in Cyprus, *Atmos Environ*, 191, 79–93, <https://doi.org/10.1016/j.atmosenv.2018.07.048>, 2018.
- 1005 Pinthong, N., Thepanondh, S., and Kondo, A.: Source Identification of VOCs and their Environmental Health Risk in a Petrochemical Industrial Area, *Aerosol Air Qual Res*, 22, 210064, <https://doi.org/10.4209/aaqr.210064>, 2022.
- Pochanart, P., Akimoto, H., Kajii, Y., Potemkin, V. M., and Khodzher, T. V.: Regional background ozone and carbon monoxide variations in remote Siberia/East Asia, *Journal of Geophysical Research: Atmospheres*, 108, <https://doi.org/10.1029/2001JD001412>, 2003.
- 1010 Pugliese, G., Ingrisch, J., Meredith, L. K., Pfannerstill, E. Y., Klüpfel, T., Meeran, K., Byron, J., Purser, G., Gil-Loaiza, J., van Haren, J., Dontsova, K., Kreuzwieser, J., Ladd, S. N., Werner, C.,



- and Williams, J.: Effects of drought and recovery on soil volatile organic compound fluxes in an experimental rainforest, *Nat Commun*, 14, 5064, <https://doi.org/10.1038/s41467-023-40661-8>, 2023.
- 1015 Ralf Koppmann: Volatile Organic Compounds in the Atmosphere, edited by: Koppmann, R., Wiley, <https://doi.org/10.1002/9780470988657>, 2007.
- Robles, H.: Acetonitrile, in: *Encyclopedia of Toxicology*, Elsevier, 28–30, <https://doi.org/10.1016/B0-12-369400-0/00015-6>, 2005.
- 1020 Salisbury, G., Williams, J., Holzinger, R., Gros, V., Mihalopoulos, N., Vrekoussis, M., Sarda-Estève, R., Berresheim, H., von Kuhlmann, R., Lawrence, M., and Lelieveld, J.: Ground-based PTR-MS measurements of reactive organic compounds during the MINOS campaign in Crete, July–August 2001, *Atmos Chem Phys*, 3, 925–940, <https://doi.org/10.5194/acp-3-925-2003>, 2003.
- Schieweck, A., Uhde, E., and Salthammer, T.: Determination of acrolein in ambient air and in the atmosphere of environmental test chambers, *Environ Sci Process Impacts*, 23, 1729–1746, <https://doi.org/10.1039/D1EM00221J>, 2021.
- 1025 Sciare J: The Agia Marina Xyliatou Observatory: A remote supersite in Cyprus to monitor changes in the atmospheric composition of the Eastern Mediterranean and the Middle East, in: *EGU General Assembly Conference Abstracts*, 2016.
- 1030 Sicre, M. A., Marty, J. C., Saliot, A., Aparicio, X., Grimalt, J., and Albaiges, J.: Aliphatic and Aromatic Hydrocarbons in the Mediterranean Aerosol, *Int J Environ Anal Chem*, 29, 73–94, <https://doi.org/10.1080/03067318708078412>, 1987.
- Sindelarova, K., Granier, C., Bouarar, I., Guenther, A., Tilmes, S., Stavrou, T., Müller, J.-F., Kuhn, U., Stefani, P., and Knorr, W.: Global data set of biogenic VOC emissions calculated by the MEGAN model over the last 30 years, *Atmos Chem Phys*, 14, 9317–9341, <https://doi.org/10.5194/acp-14-9317-2014>, 2014.
- 1035 Song, W., Williams, J., Yassaa, N., Martinez, M., Carnero, J. A. A., Hidalgo, P. J., Bozem, H., and Lelieveld, J.: Winter and summer characterization of biogenic enantiomeric monoterpenes and anthropogenic BTEX compounds at a Mediterranean Stone Pine forest site, *J Atmos Chem*, 68, 233–250, <https://doi.org/10.1007/s10874-012-9219-4>, 2011.
- 1040 Soukissian, T. and Sotiriou, M.-A.: Long-Term Variability of Wind Speed and Direction in the Mediterranean Basin, *Wind*, 2, 513–534, <https://doi.org/10.3390/wind2030028>, 2022.
- Stein, A. F., Draxler, R. R., Rolph, G. D., Stunder, B. J. B., Cohen, M. D., and Ngan, F.: NOAA's HYSPLIT Atmospheric Transport and Dispersion Modeling System, *Bull Am Meteorol Soc*, 96, 2059–2077, <https://doi.org/10.1175/BAMS-D-14-00110.1>, 2015.
- 1045 Stockwell, W. R., Kirchner, F., Kuhn, M., and Seefeld, S.: A new mechanism for regional atmospheric chemistry modeling, *Journal of Geophysical Research: Atmospheres*, 102, 25847–25879, <https://doi.org/10.1029/97JD00849>, 1997.
- 1050 Strada, S., Pozzer, A., Giuliani, G., Coppola, E., Solmon, F., Jiang, X., Guenther, A., Bourtsoukidis, E., Serça, D., Williams, J., and Giorgi, F.: Assessment of isoprene and near-surface ozone sensitivities to water stress over the Euro-Mediterranean region, *Atmos Chem Phys*, 23, 13301–13327, <https://doi.org/10.5194/acp-23-13301-2023>, 2023.
- Thunis, P., Crippa, M., Cuvelier, C., Guizzardi, D., de Meij, A., Oreggioni, G., and Pisoni, E.: Sensitivity of air quality modelling to different emission inventories: a case study over Europe, *Atmos. Environ. X*, 10, 100111, 2021.



- 1055 Tiwari, V., Hanai, Y., and Masunaga, S.: Ambient levels of volatile organic compounds in the vicinity of petrochemical industrial area of Yokohama, Japan, *Air Qual Atmos Health*, 3, 65–75, <https://doi.org/10.1007/s11869-009-0052-0>, 2010.
- Torres-Vinces, L., Contreras-Zarazua, G., Huerta-Rosas, B., Sánchez-Ramírez, E., and Segovia-Hernández, J. G.: Methyl Ethyl Ketone Production through an Intensified Process, *Chem Eng Technol*, 43, 1433–1441, <https://doi.org/10.1002/ceat.201900664>, 2020.
- 1060 Traub, M., Fischer, H., de Reus, M., Kormann, R., Heland, H., Ziereis, H., Schlager, H., Holzinger, R., Williams, J., Warneke, C., de Gouw, J., and Lelieveld, J.: Chemical characteristics assigned to trajectory clusters during the MINOS campaign, *Atmos Chem Phys*, 3, 459–468, <https://doi.org/10.5194/acp-3-459-2003>, 2003.
- 1065 Vlasenko, A., Macdonald, A. . M., Sjostedt, S. J., and Abbatt, J. P. D.: Formaldehyde measurements by Proton transfer reaction – Mass Spectrometry (PTR-MS): correction for humidity effects, *Atmos Meas Tech*, 3, 1055–1062, <https://doi.org/10.5194/amt-3-1055-2010>, 2010.
- 1070 Vrekoussis, M., Pikridas, M., Rousogenous, C., Christodoulou, A., Desservettaz, M., Sciare, J., Richter, A., Bougoudis, I., Savvides, C., and Papadopoulos, C.: Local and regional air pollution characteristics in Cyprus: A long-term trace gases observations analysis, *Science of The Total Environment*, 845, 157315, <https://doi.org/10.1016/j.scitotenv.2022.157315>, 2022.
- Wang, H., Ma, X., Tan, Z., Wang, H., Chen, X., Chen, S., Gao, Y., Liu, Y., Liu, Y., Yang, X., Yuan, B., Zeng, L., Huang, C., Lu, K., and Zhang, Y.: Anthropogenic monoterpenes aggravating ozone pollution, *Natl Sci Rev*, 9, <https://doi.org/10.1093/nsr/nwac103>, 2022a.
- 1075 Wang, L., Lun, X., Wang, Q., and Wu, J.: Biogenic volatile organic compounds emissions, atmospheric chemistry, and environmental implications: a review, *Environ Chem Lett*, 22, 3033–3058, <https://doi.org/10.1007/s10311-024-01785-5>, 2024.
- Wang, N., Edtbauer, A., Stönnner, C., Pozzer, A., Bourtsoukidis, E., Ernle, L., Dienhart, D., Hottmann, B., Fischer, H., Schuladen, J., Crowley, J. N., Paris, J.-D., Lelieveld, J., and Williams, J.: Measurements of carbonyl compounds around the Arabian Peninsula: overview and model comparison, *Atmos Chem Phys*, 20, 10807–10829, <https://doi.org/10.5194/acp-20-10807-2020>, 2020.
- 1080 Wang, S., Yuan, B., Wu, C., Wang, C., Li, T., He, X., Huangfu, Y., Qi, J., Li, X.-B., Sha, Q., Zhu, M., Lou, S., Wang, H., Karl, T., Graus, M., Yuan, Z., and Shao, M.: Oxygenated volatile organic compounds (VOCs) as significant but varied contributors to VOC emissions from vehicles, *Atmos Chem Phys*, 22, 9703–9720, <https://doi.org/10.5194/acp-22-9703-2022>, 2022b.
- 1090 Xu, Z., Zou, Q., Jin, L., Shen, Y., Shen, J., Xu, B., Qu, F., Zhang, F., Xu, J., Pei, X., Xie, G., Kuang, B., Huang, X., Tian, X., and Wang, Z.: Characteristics and sources of ambient Volatile Organic Compounds (VOCs) at a regional background site, YRD region, China: Significant influence of solvent evaporation during hot months, *Science of The Total Environment*, 857, 159674, <https://doi.org/10.1016/j.scitotenv.2022.159674>, 2023.
- Yáñez-Serrano, A. M., Nölscher, A. C., Bourtsoukidis, E., Derstroff, B., Zannoni, N., Gros, V., Lanza, M., Brito, J., Noe, S. M., House, E., Hewitt, C. N., Langford, B., Nemitz, E., Behrendt, T., Williams, J., Artaxo, P., Andreae, M. O., and Kesselmeier, J.: Atmospheric mixing ratios of methyl ethyl ketone (2-butanone) in tropical, boreal, temperate and marine environments, *Atmos Chem Phys*, 16, 10965–10984, <https://doi.org/10.5194/acp-16-10965-2016>, 2016.
- 1095 Yáñez-Serrano, A. M., Filella, I., LLusià, J., Gargallo-Garriga, A., Granda, V., Bourtsoukidis, E., Williams, J., Seco, R., Cappellin, L., Werner, C., de Gouw, J., and Peñuelas, J.: GLOVOCs -



- 1100 Master compound assignment guide for proton transfer reaction mass spectrometry users, *Atmos Environ*, 244, 117929, <https://doi.org/10.1016/j.atmosenv.2020.117929>, 2021.
- Yokelson, R. J., Goode, J. G., Ward, D. E., Susott, R. A., Babbitt, R. E., Wade, D. D., Bertschi, I., Griffith, D. W. T., and Hao, W. M.: Emissions of formaldehyde, acetic acid, methanol, and other trace gases from biomass fires in North Carolina measured by airborne Fourier transform infrared spectroscopy, *Journal of Geophysical Research: Atmospheres*, 104, 30109–30125, <https://doi.org/10.1029/1999JD900817>, 1999.
- 1105 Yuan, Q., Zhang, Z., Chen, Y., Hui, L., Wang, M., Xia, M., Zou, Z., Wei, W., Ho, K. F., Wang, Z., Lai, S., Zhang, Y., Wang, T., and Lee, S.: Origin and transformation of volatile organic compounds at a regional background site in Hong Kong: Varied photochemical processes from different source regions, *Science of The Total Environment*, 908, 168316, <https://doi.org/10.1016/j.scitotenv.2023.168316>, 2024.
- 1110 Zittis, G., Almazroui, M., Alpert, P., Ciais, P., Cramer, W., Dahdal, Y., Fnais, M., Francis, D., Hadjinicolaou, P., Howari, F., Jrrar, A., Kaskaoutis, D. G., Kulmala, M., Lazoglou, G., Mihalopoulos, N., Lin, X., Rudich, Y., Sciare, J., Stenchikov, G., Xoplaki, E., and Lelieveld, J.: Climate Change and Weather Extremes in the Eastern Mediterranean and Middle East, *Reviews of Geophysics*, 60, <https://doi.org/10.1029/2021RG000762>, 2022.
- 1115